

AD 744711

INVESTIGATIONS TO UNDERSTAND THE PLASTIC DEFORMATION AND STRENGTHENING MECHANISMS OF SOLID SOLUTION PHASES OF TITANIUM

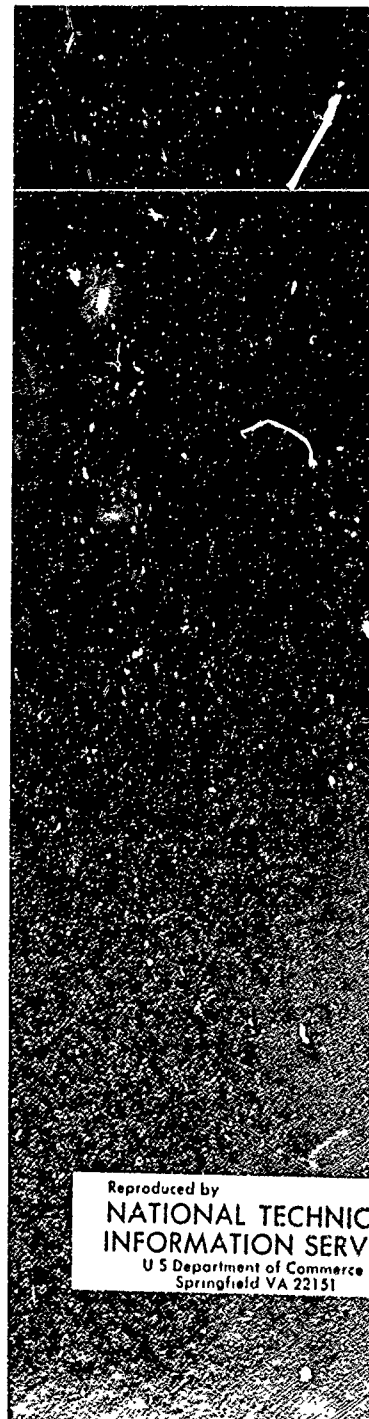
by
H. Conrad,
M. Doner,
and
B. de Meester
Department of
Metallurgical Engineering
and
Materials Science

TECHNICAL REPORT UKY 50-72-MET 15
MAY 1972

AIR FORCE TECHNICAL REPORT
AFML-TR-72-04

APPROVED FOR PUBLIC RELEASE;
DISTRIBUTION UNLIMITED

Air Force Materials Laboratory
Air Force Systems Command
Wright-Patterson Air Force Base, Ohio



Reproduced by
NATIONAL TECHNICAL
INFORMATION SERVICE
U S Department of Commerce
Springfield VA 22151

COLLEGE
OF
ENGINEERING
UNIVERSITY OF KENTUCKY

62

NOTICE

When Government drawings, specifications, or other data are used for any purpose other than in connection with a definitely related Government procurement operation, the United States Government thereby incurs no responsibility nor any obligation whatsoever; and the fact that the government may have formulated, furnished, or in any way supplied the said drawings, specifications, or other data is not to be regarded by implication or otherwise as in any manner licensing the holder or any other person or corporation, or conveying any rights or permission to manufacture, use, or sell any patented invention that may in any way be related thereto.

* * *

Copies of this report should not be returned unless return is required by security considerations, contractual obligations, or notice on a specific document.

COLLEGE ADMINISTRATION

DR. R. M. DRAKE, JR.
DEAN, COLLEGE OF ENGINEERING

DR. J. E. FUNK
ASSOCIATE DEAN

PROF. D. K. BLYTHE
ASSOCIATE DEAN

PROF. W. W. WALTON
ASSISTANT DEAN

DR. B. F. PARKER
AGRICULTURAL ENGINEERING

DR. R. B. GRIEVES
CHEMICAL ENGINEERING

DR. S. F. ADAMS
CIVIL ENGINEERING

DR. EARL L. STEELE
ELECTRICAL ENGINEERING

DR. DONALD C. LEIGH
ENGINEERING MECHANICS

DR. R. EICHORN
MECHANICAL ENGINEERING

DR. H. CONRAD
METALLURGICAL ENGINEERING
AND MATERIALS SCIENCE

OFFICE OF RESEARCH AND ENGINEERING SERVICES

ROBERT M. DRAKE, JR., Ph.D.
DIRECTOR AND DEAN OF THE
COLLEGE OF ENGINEERING

RUSSELL E. PUCKETT, M.S.
ASSOCIATE DIRECTOR

R. WILLIAM DEVORE, M.A.
DIRECTOR OF PUBLICATION SERVICES

For additional copies or information
address correspondence to:

ORES Publications
College of Engineering
University of Kentucky
Lexington, Kentucky 40506

A PUBLICATION OF THE OFFICE OF RESEARCH AND ENGINEERING SERVICES

INVESTIGATIONS TO UNDERSTAND THE PLASTIC
DEFORMATION AND STRENGTHENING MECHANISMS
OF SOLID SOLUTION PHASES OF TITANIUM

by

H. Conrad

M. Doner

and

B. de Meester

Department of Metallurgical Engineering
and Materials Science

Air Force
TECHNICAL REPORT AFML-TR-72-84

MAY 1972

APPROVED FOR PUBLIC RELEASE; DISTRIBUTION UNLIMITED

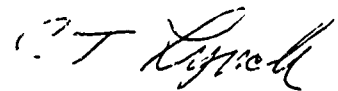
AIR FORCE MATERIALS LABORATORY
AIR FORCE SYSTEMS COMMAND
WRIGHT-PATTERSON AIR FORCE BASE, DAYTON, OHIO

I

This report was prepared by the Metallurgical Engineering and Materials Science Department, College of Engineering, University of Kentucky, Lexington, Kentucky, under contract F33615-68-C-1052. The contract was initiated under Project No. 7351 and Task No. 735103. The work was administered by the Air Force Materials Laboratory, Air Force Systems Command, Wright-Patterson Air Force Base, Ohio, with Dr. H. L. Gegel acting as Project Engineer.

This technical report covers the period from February 1968 to May 1971.

This report has been reviewed and is approved.



C.T. LYNCH, Chief
Advanced Metallurgical Studies
Branch
Metals and Ceramics Division

ABSTRACT

The plastic flow and fracture of titanium are reviewed with special attention to the mechanisms which are controlling. The low temperature ($T < 0.3T_m$) plastic deformation is described by

$$\tau = \tau^* (T, \dot{\gamma}, C_i) + 0.5\mu b \rho^{\frac{1}{2}} + \tau_{\mu} (C_s)$$

where τ is the resolved shear stress, T the temperature, $\dot{\gamma}$ the strain rate, C_i the interstitial solute content, μ the modulus, b the Burgers vector, ρ the dislocation density and C_s the substitutional solute content. For α -stabilizing substitutional solutes

$$\tau_{\mu} (C_s) = 34.1 \quad I C_{\alpha}^{\frac{1}{2}} \quad (\text{Kg/mm}^2)$$

where I is the interaction parameter derived from individual atomic interaction coefficients. The rate controlling dislocation mechanism for both unalloyed titanium and titanium alloys at low temperatures is the thermally activated overcoming of interstitial solute obstacles. Fracture at low temperatures is most generally of the shear type and appears to be controlled by the same mechanism as plastic flow.

Static and dynamic strain aging occurs in the intermediate temperature range of 0.3 to 0.45 T_m . At higher temperatures the deformation can be described very well by Weertman's dislocation climb model. Fracture at high temperatures appears to be controlled by the same mechanism.

The ratio of fatigue limit to yield stress is approximately 0.65, relatively independent of grain size, interstitial content and temperature, suggesting that fatigue is controlled by the same mechanism as plastic flow.

TABLE OF CONTENTS

	Page
Introduction	1
Plastic Flow	3
1. Single Crystals	3
a. Deformation Modes	3
b. Effects of Temperature and Interstitial Content on the Resolved Shear Stress for Slip and Twinning	5
c. Deformation Kinetics	7
d. Strain Hardening	10
2. Polycrystals	12
a. Characterization of Structure	12
b. Taylor Factor	15
c. Effects of Temperature, Interstitial Content and Grain Size on the Stress-Strain Behavior	15
d. Deformation Kinetics at Low Temperatures ($T < 0.3T_m$)	22
e. Athermal Component at Low Temperatures ($T < 0.3T_m$)	26
f. Role of Twinning	32
g. Deformation at High Temperatures ($T < 0.4T_m$)	33
Fracture	34
1. Unidirectional Stressing: Tension	34
a. Fracture Modes at Low Temperatures	34
b. Effects of Temperature, Grain Size and Solute Content on the Fracture Behavior at Low Temperatures ($T < 0.3T_m$)	36
c. Fracture at High Temperatures ($T > 0.4T_m$)	39
2. Fatigue	39
Acknowledgement	43
References	45
Publications	51
1. Scientific Journals	51
2. Theses	53

List of Figures

Fig.		Page
1.	Effect of temperature on the various elastic constants in titanium. Data from Refs. 5 and 6.	2
2.	The effects of temperature and interstitial content on the critical resolved shear stress for prism slip. Data from Refs. 16, 17, 22-27.	6
3.	τ_{crss} versus $T^{\frac{1}{2}}$ for prism slip in unalloyed titanium as a function of interstitial content. Data from Ref. 25 and 27.	8
4.	The effect of temperature on τ_{crss} for basal slip, the shear stress for twinning on the $\{10\bar{1}2\}$, $\{11\bar{2}1\}$, $\{11\bar{2}2\}$ and $\{10\bar{1}1\}$ planes, τ_{crss} for prism slip and shear stress for $\{10\bar{1}0\} \frac{1}{3} \langle 11\bar{2}0 \rangle$ edge dislocation velocity of 10^{-3} cm sec $^{-1}$. Data from Refs. 16, 17, 22-27, 30, 31.	9
5.	The activation enthalpy for basal and prism slip versus the temperature. Data from Refs. 24-27.	11
6.	Common textures in titanium sheet and rod or wire. Data from Refs. 14, 18, 39-41.	14
7.	Comparison of the effect of temperature on the flow stress of polycrystalline specimens with that for prism slip in single crystals and for the stress at which $\{10\bar{1}0\} \frac{1}{3} \langle 11\bar{2}0 \rangle$ edge dislocations move at a velocity of $\sim 10^3$ cm sec $^{-1}$. From Okazaki and Conrad (46).	16
8.	Stress-strain curves for unalloyed titanium (0.5 at.% Oeq) with 22 microns grain size as a function of temperature. Data from Refs. 10 and 40.	17
9.	Effects of temperature, grain size and interstitial content on the 0.2% yield stress. Data from Refs. 10, 27, 40 and 46.	19
10.	Effect of temperature and strain rate on the strain hardening of titanium (0.5 at.% Oeq) with 16 micron grain size. From Santhanam and Reed-Hill (50).	20

Fig.	Figures (Continued)	Page
11.	τ^* at 4.2°K and 300°K versus the square root of the interstitial solute content for unalloyed titanium and some titanium alloys. Data from Refs. 27, 46, 58-61.	23
12.	Activation enthalpy versus temperature for the deformation of unalloyed titanium and some alloys. Data from Refs. 27, 46, 58, 60, 61.	25
13.	Force-activation distance curve for the deformation of unalloyed titanium at low temperatures. From Okazaki and Conrad (46).	27
14.	Flow stress versus the square root of the dislocation density in A-70 titanium (1.0 at.% Oeq) as a function of grain size and temperature. From Conrad et al. (54).	28
15.	Tensile strength at room temperature versus square root of the atomic fraction of α -stabilizing solutes. From Gegel (75).	30
16.	$d\sigma/dc^{\frac{1}{2}}$ versus the interaction parameter defined as the sum of the square roots of the absolute values of the individual interaction coefficients expressed in eV per atom. From Gegel (75).	31
17.	$\log \frac{kT}{D\mu b}$ versus $\log \sigma/\mu$ for the deformation of α - and β -titanium at high temperatures. Data from Refs. 84 - 86.	35
18.	Effects of temperature, solute content and grain size on the fracture stress of titanium. Data from Refs. 40, 58, 91.	37
19.	Effects of the interstitials C, O and N on the total elongation at fracture at 300°K. Data from Ref. 94-96.	38
20.	Effects of temperature and strain rate on the total elongation at fracture in commercial purity titanium (~0.5 at.% Oeq) sheet of 16 micron grain size. From Santhanam and Reed-Hill (50).	40
21.	Effect of interstitial content on S-N curves of unalloyed titanium with 32 micron grain size at 300°K. Interstitial contents in terms of Oeq are: Ti 160 (1.1at%), Ti 120 (0.4 at%) and H.P.Ti (0.3at%). From Turner and Roberts (100).	41

Fig.	Figures (Continued)	Page
22.	Ratio of the fatigue limit to the yield stress in unalloyed titanium at 300°K as a function of interstitial content and grain size. Data from Refs. 98-104.	42
23.	Ratio of stress to cause failure at 10^5 cycles to the yield stress and ratio of the fatigue limit to the yield stress for unalloyed titanium as a function of temperature. Data from Refs 99, 100 and 103.	44

INTRODUCTION

This paper is a review of the present state of our understanding of the plastic flow and fracture of titanium. Special attention is given to identifying the dislocation mechanisms which are operative and controlling. It is felt that an understanding of the mechanical behavior of titanium in terms of recent advances in dislocation theory and materials science will provide a base for the more effective use of available alloys and the design of new and improved alloys.

Of importance to the mechanical behavior of titanium are certain physical properties. Melting occurs at 1941°K and a phase change from BCC to CPH crystal structure takes place at 1156°K (1). The Debye temperature is reported to be 402° to 428°K (2, 3, 4) yielding a Debye frequency of approximately $9 \times 10^{12} \text{ sec}^{-1}$. Some of the other physical properties of importance are the effect of temperature on the elastic moduli (Fig. 1) and diffusion coefficients, Tables I and II[†]. From Fig. 1 it is seen that the moduli of titanium exhibit a relatively strong temperature dependence. In general, both interstitial and α -stabilizing substitutional solutes tend to increase the elastic moduli (3, 4, 7, 9); their effect on the temperature dependence is not completely clear, but they do not appear to alter it significantly. The addition of β -stabilizing solutes generally leads to a decrease in modulus (4).

Table I. Diffusion of Interstitial Solutes in α -Titanium (10)

Interstitial Solute	D_0	Q
	cm^2/sec	Kcal/mole
O	0.78 - 16	45 - 52.5
N	0.2 - 6.8	57 - 68
C	5.1	43.5 - 48.5
H	0.3 - 0.9	12.4 - 14.7

[†] The diffusion coefficients listed in Tables I and II are those considered to be the most realistic (10).

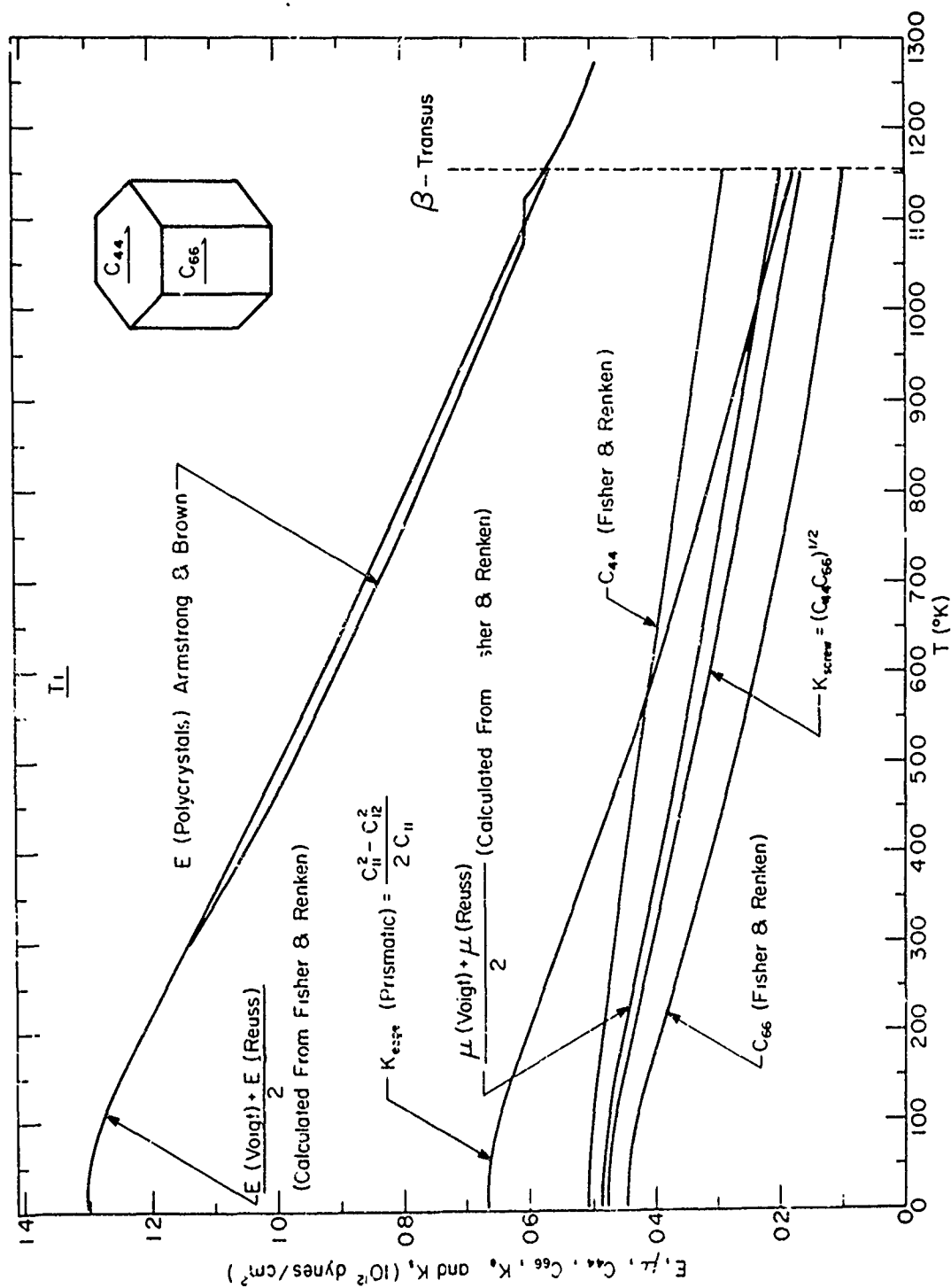


Fig. 1. Effect of temperature on the various elastic constants in titanium. Data from Refs. 5 and 6

An excellent review of the crystallography and deformation modes in titanium and other CPH metals is provided by Partridge (11). The effects of interstitial solutes on the lattice parameters

Table II. Self-Diffusion and Substitutional Solute Diffusion in Titanium (10)

Atom Species	D_{o_1} cm ² /sec	Q_1 Kcal/mole	D_{o_2} cm ² /sec	Q_2 Kcal/mole
<u>α-Ti</u>				
Self	-	58 [†]	-	-
	-	71.3 ^{††}	-	-
<u>β-Ti</u>				
Self	1.1	60	3.6×10^{-4}	31.2
Substitutional Solute	0.2-20	51-73	3×10^{-4} - 80×10^{-4}	29-43

Note: Two values of D_o and Q are given because of curvature in the Arrhenius plots. The subscript 1 refers to the high temperature results, the subscript 2 to low temperature data.

* Energy for the formation of vacancies plus that for migration determined from the recovery of electrical resistivity after plastic deformation: private communication K. Okazaki.

†† Twice the energy to form vacancies determined from heat capacity measurements: V. O. Shestopol, Soviet Phys. Solid State 7 232 (1966).

of CPH titanium are reviewed by Tyson (12); the elastic properties of dislocations in titanium are described by Teutonico (13).

Plastic Flow

1. Single Crystals

a. Deformation Modes (11, 14): Numerous investigators have established that the most common slip modes in CPH α -titanium are (in order of ease of operation) the $\{10\bar{1}0\}$, $\{10\bar{1}1\}$ and $\{0001\}$ planes

with the \vec{a} direction, $\langle 11\bar{2}0 \rangle$, as the slip direction. This order seems to prevail over the entire temperature range of the CPH structure; however, slip on the $\{10\bar{1}1\}$ and the (0001) planes tends to become relatively more favorable compared to the $\{10\bar{1}0\}$ planes as the interstitial solute content or the temperature is increased. These three planes with the slip vector in the basal plane constitute a total of four independent slip systems. Evidence for slip with a vector out of the basal plane has been obtained by electron transmission microscopy (15-17) and by slip trace analysis (15, 17).

The dislocation structure in deformed titanium single crystals was studied by Cass (16). For specimens deformed by prism slip and sectioned parallel to the prism plane the structure consisted of long lengths of single dislocation lines, most of them very near to the screw orientation. These screw dislocations trailed a large number of resolvable and, presumably, unresolvable dipoles. In one specimen, dislocations with a vector out of the basal plane (presumably $\vec{c} + \vec{a}$) were observed. For specimens deformed by basal glide and sectioned parallel to the basal plane, the dislocations were again near the screw orientation and as in the prism case, there was no tendency for pairing or tangling of long dislocations. However, the isolated debris appeared to be in the form of small, approximately circular loops rather than elongated ones.

Although the slip systems operative in unalloyed single crystals of BCC β -titanium have not been established, it is expected that they are the same as those for other metals of the BCC structure, i.e. $\{110\}$, $\{112\}$ and $\{123\}$ planes with $\langle 111 \rangle$ as the slip direction (18). For the stable BCC alloys of titanium with vanadium (20 to 50 at. %V) and with molybdenum (15 at. %) the slip direction was found to be $\langle 111 \rangle$ with $\{110\}$, $\{112\}$ and $\{123\}$ as possible slip planes (19, 20).

Twinning in titanium has been reported to occur on the $\{10\bar{1}x\}$ and $\{11\bar{2}x\}$ planes (11, 14, 17). The particular twinning plane which is operative in a given case is dependent on the direction of stressing with

respect to the crystallographic axes and on the temperature. In general, the tendency for twinning decreases with increase in temperature and in interstitial solute content. However, Paton and Backofen (17) found that the stress for the $\{10\bar{1}1\}$ twinning mode decreased with increase in temperature. The magnitude of the shear associated with several twinning planes is given in Table III.

Table III. Twinning Shear in Titanium

Plane	Direction	Magnitude of Shear			
		Calculated	Ref.	Observed	Ref.
$\{10\bar{1}1\}$	$\langle 10\bar{1}2 \rangle$	0.104	17	0.09 to 0.11	17
$\{11\bar{2}1\}$	$\langle 11\bar{2}6 \rangle$	0.638	11	---	--
$\{11\bar{2}2\}$	$\langle 11\bar{2}3 \rangle$	0.218	21	0.21	17
$\{11\bar{2}2\}$	$\langle 11\bar{2}3 \rangle$	0.225	11	---	--

b. Effects of Temperature and Interstitial Solute Content on the Resolved Shear Stress for Slip and Twinning: The effects of temperature T and interstitial solute content C_i on the critical resolved shear stress τ_{crss} (resolved shear strain γ equal to $\sim 10^{-4}$) for $\{10\bar{1}0\} \langle 11\bar{2}0 \rangle$ prism slip are presented in Fig. 2. The total C + N + O interstitial solute content is given in terms of an oxygen equivalent (25), with $C = \frac{3}{4} O$ and $N = 2 O_h$. The effect of temperature on the τ_{crss} for a given interstitial content is typical, permitting the separation of the flow stress into a thermal component τ^* and an athermal component τ_μ (29). The interstitial content influences both τ^* and τ_μ , the effect on τ^* increasing with decrease in temperature. The effect of the resolved shear strain γ on the flow stress is primarily through τ_μ (25,27). Moreover, over the temperature range of 0°K to 650°K the strain hardening coefficient $\theta = d\tau/d\gamma$ divided by the shear modulus μ (C_{66}) is relatively independent of temperature (25,27). Thus, one can write for the resolved shear stress for prism slip,

$$\tau = \tau^*(T, \dot{\gamma}, C_i) + \tau_\mu(\mu, \gamma, C_i); \quad T_0 (\tau^* = 0) = 600^\circ K \quad (1)$$

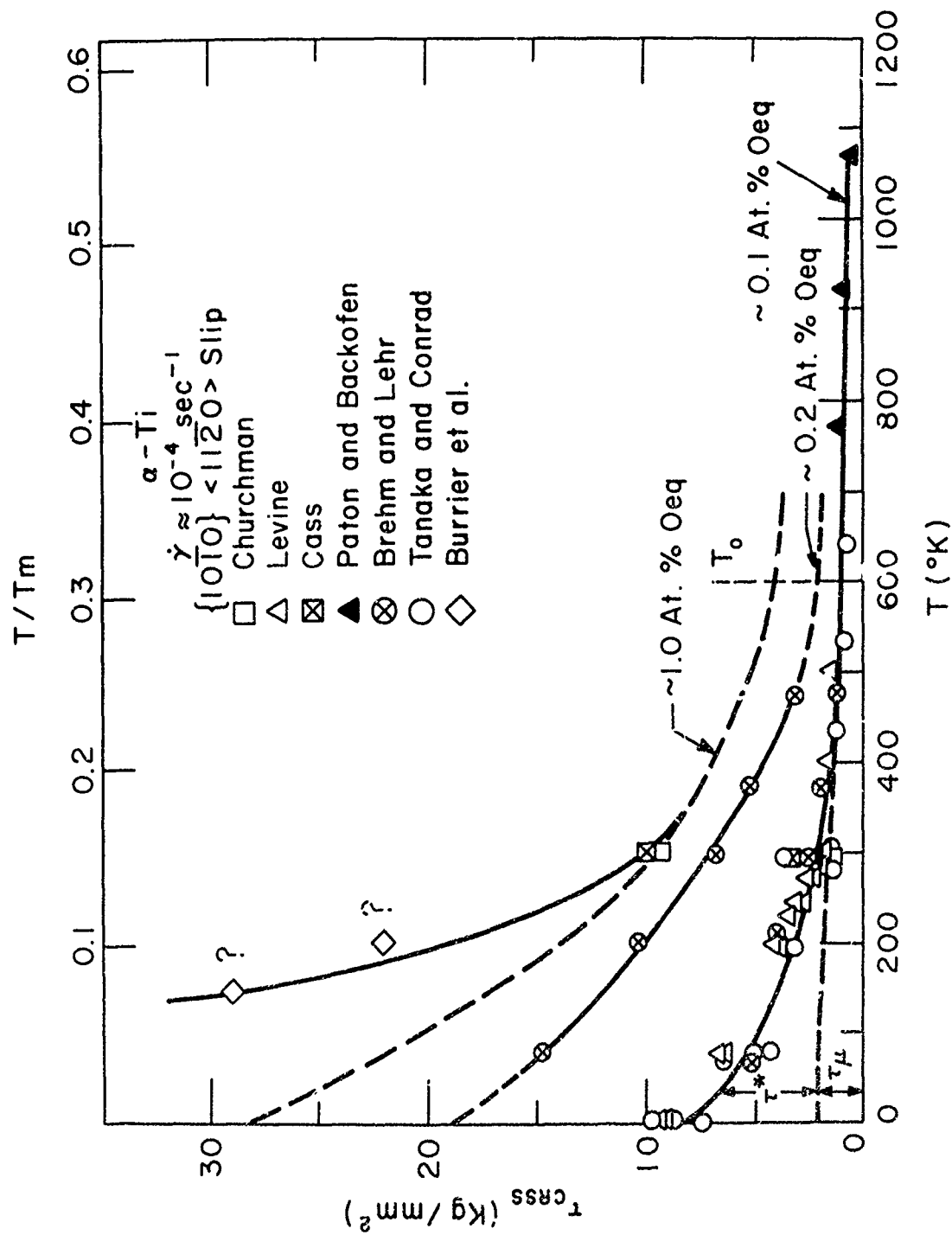


Fig. 2. The effects of temperature and interstitial content on the critical resolved shear stress for prism slip. Data from Refs. 16, 17, 22-27.

where $\dot{\gamma}$ is the resolved shear strain rate. τ^* decreases in an approximately linear fashion with the square root of the temperature (Fig. 3) yielding

$$\tau^* \approx \tau_O^* - a T^{\frac{1}{2}}; \quad T_O^* (\tau^* \approx 0.1 \text{ Kg/mm}^2) = 510^\circ\text{K} \quad (2)$$

The values of τ_O^* and a are proportional to the square root of the interstitial content with $\tau_O^* = 0.06\mu_O C_i^{\frac{1}{2}}$ and $a = 11 C_i^{\frac{1}{2}} \text{ Kg/mm}^2/^\circ\text{K}^{\frac{1}{2}}$.

Using the etch pit technique, Tanaka and Conrad (30) investigated the motion of $\{10\bar{1}0\}^{\frac{1}{2}} \langle 11\bar{2}0 \rangle$ edge dislocations in zone refined single crystals with an interstitial content of $\sim 0.1 \text{ at.}\% \text{ C}$. The stress associated with a dislocation velocity of $\sim 10^{-3} \text{ cm sec}^{-1}$ is plotted as a function of temperature in Fig. 4. There is good agreement between this stress and τ_{crss} for prism slip at a strain rate of about 10^{-4} sec^{-1} .

Also shown in Fig. 4 is the effect of temperature on the τ_{crss} for basal slip and on the shear stresses for twinning on the $\{10\bar{1}2\}$, $\{11\bar{2}1\}$, $\{11\bar{2}2\}$ and $\{10\bar{1}1\}$ planes. It is seen that the temperature dependence of τ_{crss} for basal slip is appreciably higher than that for prism slip, but the effect of interstitial content on the temperature dependence appears to be less. The stress for twinning on the $\{10\bar{1}2\}$, $\{11\bar{2}1\}$ and $\{11\bar{2}2\}$ planes increases with temperature while that for $\{10\bar{1}1\}$ twinning decreases. The stress for twinning on the former three planes is less than that for prism slip below about 200°K , but it is above at 300°K and higher. The crossover for basal slip is somewhere between 300° and 400°K .

c. Deformation Kinetics: It has been shown (27) that the deformation kinetics for prism slip in unalloyed titanium are described by

$$\dot{\gamma} = \rho_m b \bar{v} = A \exp - \{G(\tau^*)/kT\} \quad (3)$$

$$= \frac{\rho_m}{l^*} A_s b v^* \exp (S/k) \exp \{-H(\tau^*)/kT\} \quad (3a)$$

$$= v \exp \{-H(\tau^*)/kT\} \quad (3b)$$

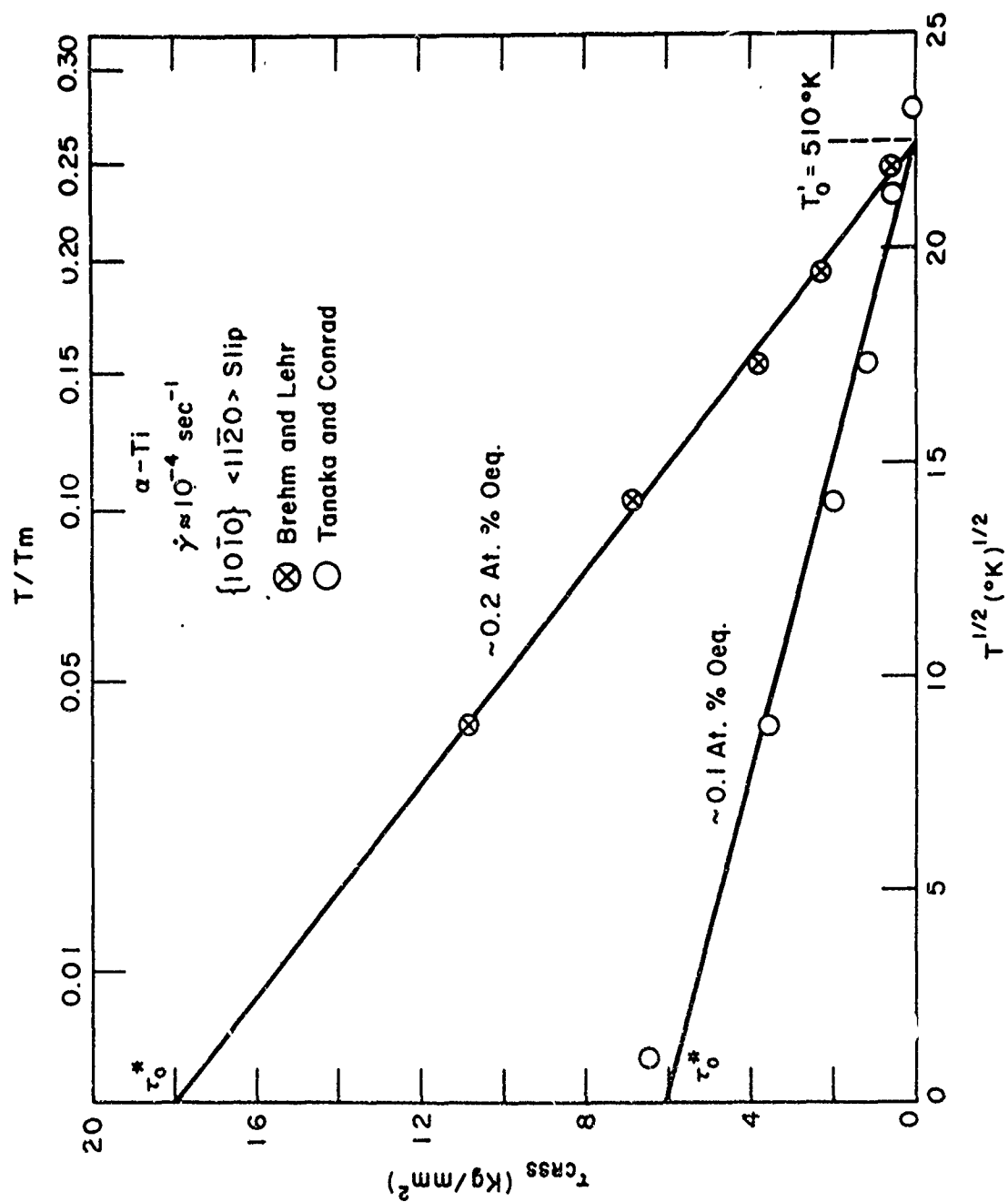


Fig. 3. τ_{crss} versus $T^{-1/2}$ for prism slip in unalloyed titanium as a function of interstitial content. Data from Ref. 25 and 27.

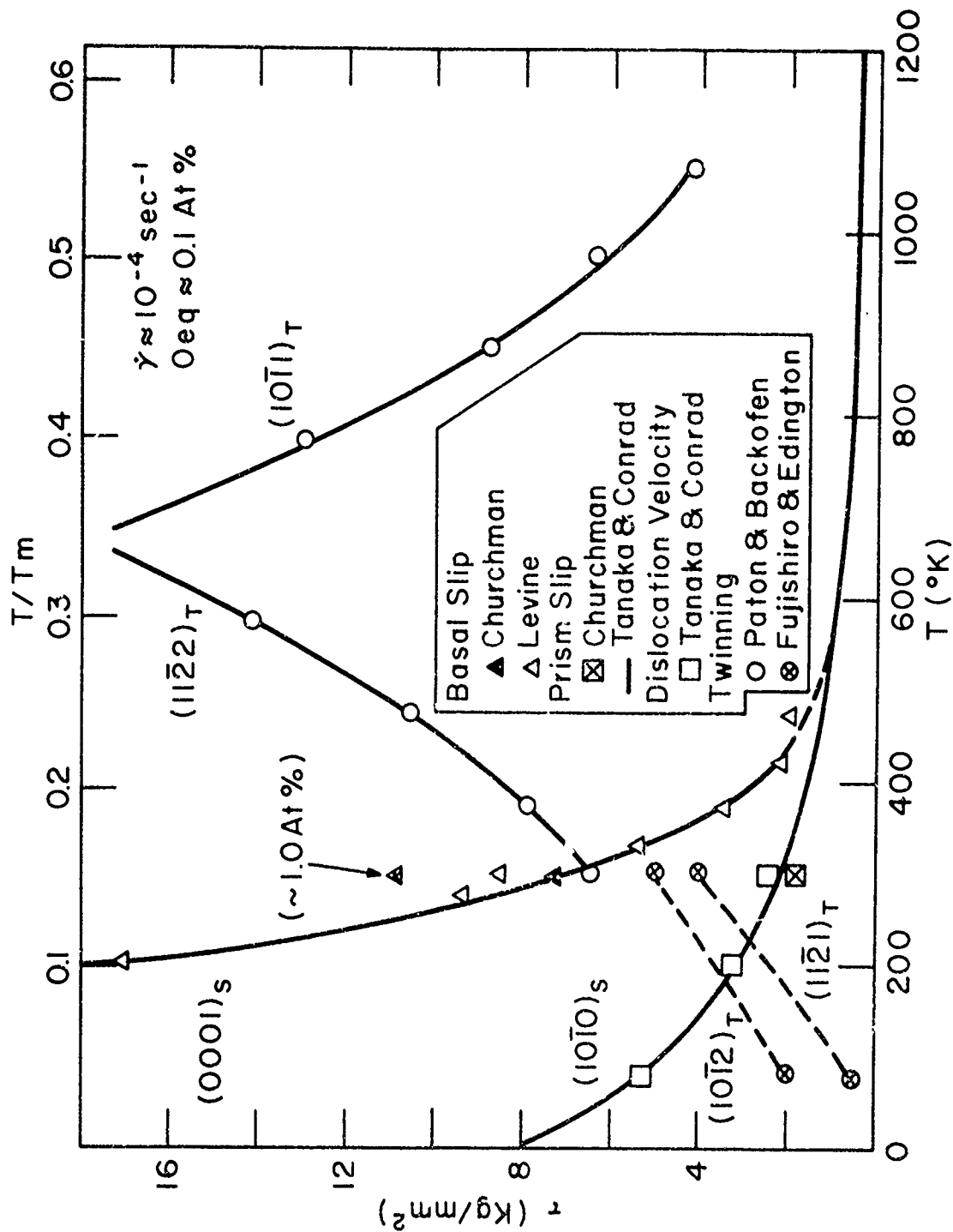


Fig. 4. The effect of temperature on τ_{crss} for basal slip, the shear stress for twinning on the $\{10\bar{1}2\}$, $\{11\bar{2}1\}$, $\{11\bar{2}2\}$ and $\{10\bar{1}1\}$ planes, τ for prism slip and shear stress for $\{10\bar{1}0\}$ & $\langle 11\bar{2}0 \rangle$ edge dislocation velocity of $10^{-3} \text{ cm sec}^{-1}$. Data from Refs. 16, 17, 22-27, 30, 31.

where $\dot{\gamma}$ is the shear strain rate, ρ_m the mobile dislocation density, b the Burgers vector, \bar{v} the average dislocation velocity, G the Gibbs free activation energy, A a constant, ℓ^* the average spacing between obstacles along the mobile dislocations, A_s the area of the slip plane swept out per successful thermal fluctuations, ν^* the vibrational frequency of the dislocation segment involved in the thermal activation and k and T have their usual meaning. $G = H - TS$ where H is the activation enthalpy and S is the activation entropy.

Plots of H versus T for prism and basal slip are given in Fig. 5. H was derived from constant strain rate type tests using the relationships developed by Conrad and Wiedersich (32). To be noted is that $H_{T_0}' = 1.25$ eV ($0.29 \mu b^3$) for prism slip ($\mu = C_{88}$) independent of interstitial content and 2.34 eV ($0.33 \mu b^3$) for basal slip ($\mu = C_{44}$). H_{T_0}' for prism slip in titanium is similar in magnitude ($0.2 \mu b^3 - 0.3 \mu b^3$) to that observed for prism slip in the CPH metals Cd, Zn and Be (12, 33, 34). Considering Eqn. 3b, the slopes of the curves of Fig. 5 yield $\nu = 3.3 \times 10^8 \text{ sec}^{-1}$ and $5.2 \times 10^{26} \text{ sec}^{-1}$ respectively for prism and basal slip. The value of ν for prism slip is within the range of values (10^1 to 10^{15} sec^{-1}) generally obtained for the deformation of metals at low temperatures (33-35), while that for basal slip is considerably higher, casting some suspicion on the validity of the analysis for basal slip.

A consideration of the data in Figs. 2 to 5, and other results (27, 30), along with the results on polycrystalline specimens to be discussed below, leads to the conclusion that stress-assisted, thermally activated overcoming of interstitial solute obstacles by moving edge dislocations is the rate controlling mechanism for prism slip in titanium at low temperatures ($T < 0.3T_m$). In the cases of basal slip and twinning, there are at present insufficient data to permit an identification of the mechanisms which are controlling.

d. Strain Hardening: The strain hardening coefficient θ for prism slip was found to vary with temperature approximately as the

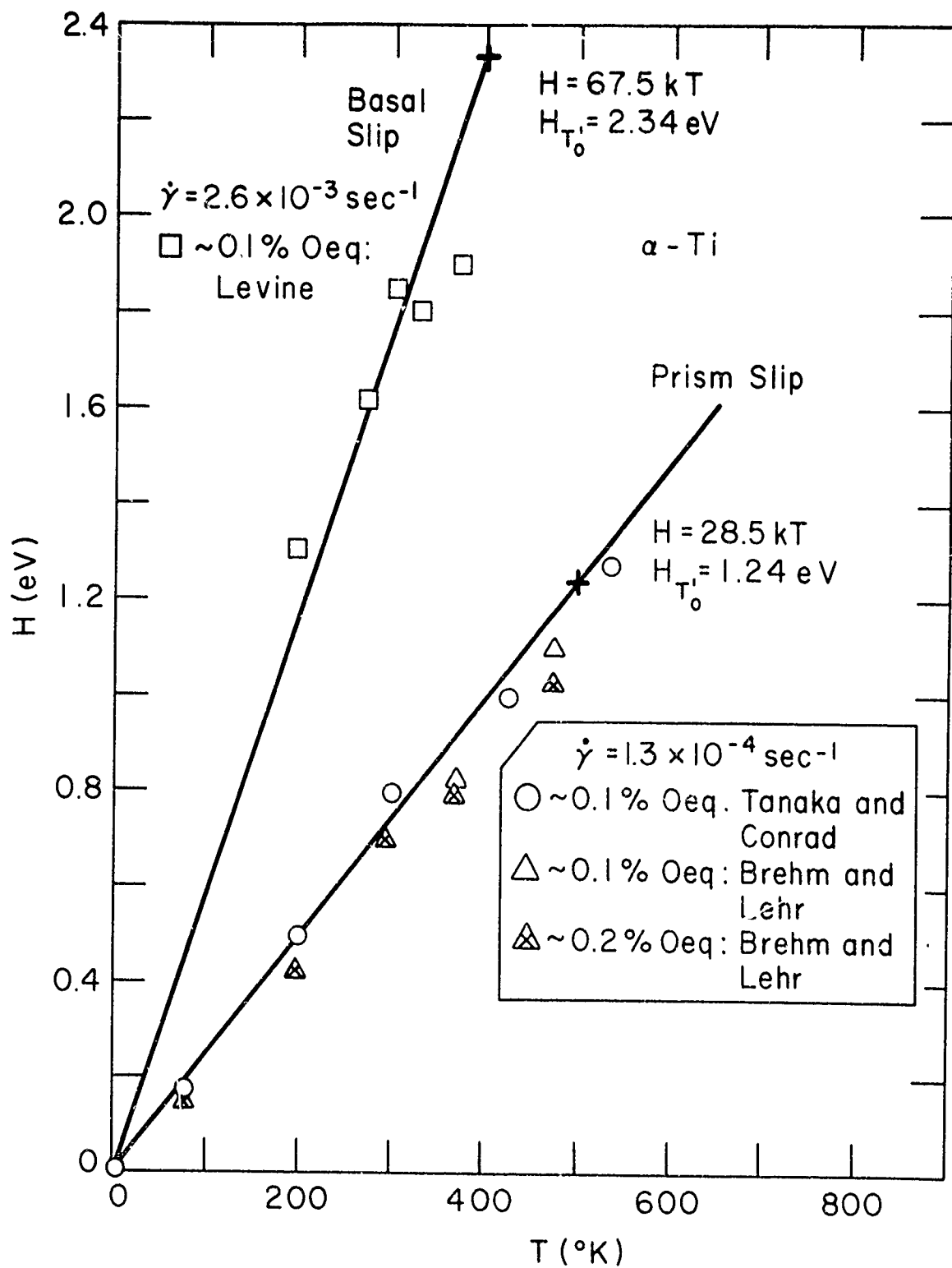


Fig. 5. The activation enthalpy for basal and prism slip versus the temperature. Data from Refs. 24-27.

shear modulus $\mu = C_{33}$ over the temperature range of 78° to 650°K with $\theta/\mu \approx 10^{-3}$ (25,27). A slight increase in θ/μ did, however, occur at 4.2°K (27). The magnitude of the strain hardening in titanium is similar to that reported for prism slip in other CPH metals (33,34). It is about an order of magnitude larger than that generally found for Stage I of basal slip in CPH metals or easy glide in cubic metals, being more nearly that for Stage II of basal slip (27). A comparison of the dislocation density measurements on titanium single crystals (16) with predictions based on the observed strain hardening during prism slip suggests that cutting of forest dislocations may be the mechanism responsible for strain hardening on this slip system (27). No data are available on the strain hardening associated with basal slip in titanium.

2. Polycrystals

a. Characterization of Structure: Important to understanding the mechanical behavior of single-phase polycrystalline titanium is a knowledge of the "character" of the structure, i.e. the grain size, shape and distribution, the texture and the initial dislocation structure. A detailed characterization of the recrystallized structure of swaged and annealed titanium (0.1 at.% to 1.0 at.% Oeq) wires with 1 to 20 microns average grain size was carried out by Okazaki and Conrad (37, 38). In summary, quantitative optical microscopy (including serial sectioning) established that: (a) the grains are relatively equiaxed in all three dimensions, (b) the three dimensional grain size distribution is approximately log-normal, (c) the grains become more regular in shape with increase in grain size and (d) the grain size distribution for a given average grain size is independent of the combination of time and temperature used to obtain the grain size. Texture studies established that for grain sizes of about 1 to 2 microns there exists a strong texture of the $[10\bar{1}0]$ direction in the basal plane parallel to the wire axis. This splits into two $[10\bar{1}0]$ components, each about 15° from the wire axis, for grain sizes of 5 microns and larger, the intensity of these components tending to decrease with increase in grain size. The

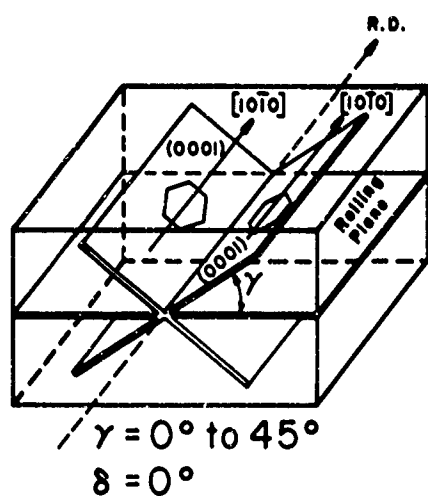
initial dislocation density increased with decrease in grain size and increase in interstitial content, ranging from 10^7 to 10^9 cm^{-2} .

The textures commonly observed in titanium sheet and rod or wire are illustrated in Fig. 6 (14, 18, 39-41). The texture of cold-rolled unalloyed sheet is most generally one with the $[10\bar{1}0]$ direction parallel to the rolling direction and the basal plane tilted about 20° to 40° to the plane of the sheet. Upon recrystallizing, the texture initially sharpens for fine grain sizes (1 to 2 microns). For larger grain sizes (> 5 microns) there occurs a rotation of the basal plane, so that the $\langle 11\bar{2}0 \rangle$ direction becomes more nearly parallel to the rolling direction, although this direction may still be inclined to the rolling plane. For both the cold rolled and the recrystallized textures, interstitial and substitutional solutes tend to reduce the angle γ between the basal plane and the plane of the sheet, yielding in extreme cases a texture with the basal plane in the plane of the sheet. Hot working yields textures similar to those of the large grain size recrystallized material; it may also yield textures with the basal plane parallel to the plane of the sheet.

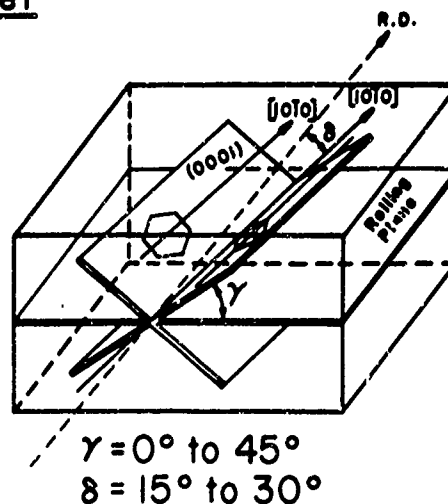
The texture of cold worked rod or wire consists of the $[10\bar{1}0]$ direction parallel to the rod or wire axis. Similar to sheet, a sharpening of cold worked texture occurs upon recrystallizing to a fine grain size. For the larger grain sizes, the basal plane becomes tilted about 10° to 15° to the wire axis and it rotates about the c-axis so that the $\langle 11\bar{2}0 \rangle$ direction now becomes the projection of the wire axis on the basal plane.

Employing the method of Calnan and Clews (42), a theoretical deformation process which resulted in the experimentally observed deformation textures in titanium was developed by Williams and Eppelsheimer (43). This deformation process required the combined operation of three slip systems, $(0001) \langle 11\bar{2}0 \rangle$, $\{10\bar{1}1\} \langle 11\bar{2}0 \rangle$ and $\{10\bar{1}0\} \langle 11\bar{2}0 \rangle$ and two types of twinning, $\{10\bar{1}2\}$ and $\{11\bar{2}2\}$. From their analysis, the authors found that the critical shear stress for slip and for twinning at 300°K were related in the following manner:

Sheet

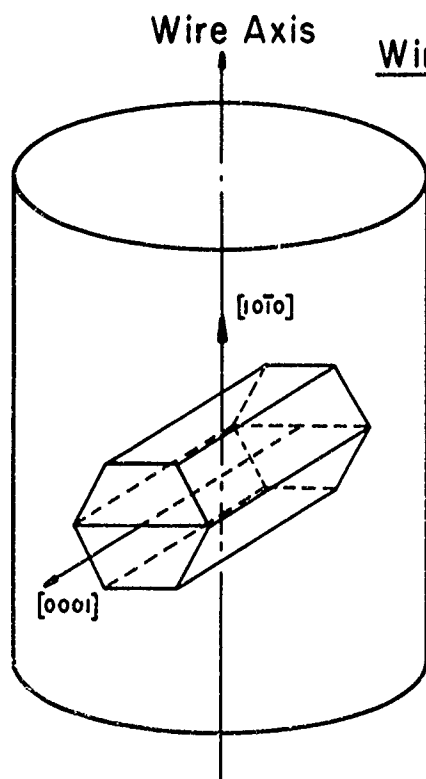


Cold Rolled; Annealed Fine
Grain Size

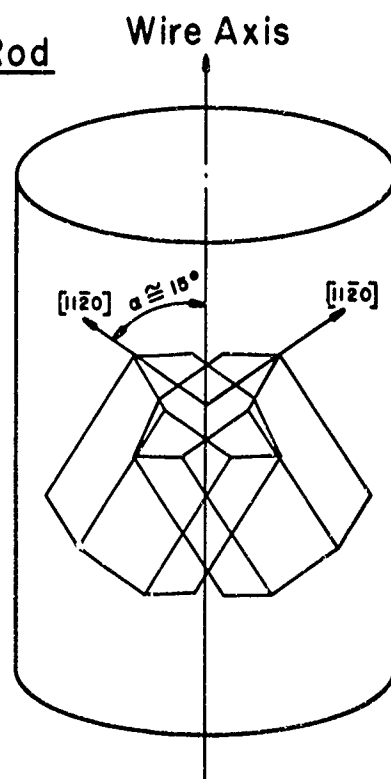


Annealed Large Grain Size;
Hot Worked

Wire or Rod



Cold Worked; Annealed
Fine Grain Size



Annealed Large Grain
Size; Hot Worked

Fig. 6. Common textures in titanium sheet and rod or wire. Data from
Refs. 14, 18, 39-41.

$$\tau_s \{00\bar{1}1\} = 1.1 \tau_s \{10\bar{1}1\} = 1.02 \tau_s \{10\bar{1}0\} = \tau_T \{10\bar{1}2\} = \tau_T \{11\bar{2}2\}.$$

These ratios are in reasonable accord with the measured stresses for slip and twinning at 300°K depicted in Fig. 4.

b. Taylor Factor: To interpret the mechanical behavior of polycrystals in terms of slip in single crystals one needs to know the value of the Taylor factor \bar{M} relating the tensile flow stress of polycrystalline specimens to the resolved shear stress for slip in single crystals. Armstrong et al. (44) estimated \bar{M} for CPH metals to be about 4 from the effect of grain size on the flow stress. Employing a Sachs-type (45) analysis they obtained a value of 6.5 for CPH metals with basal slip. Conrad and coworkers (27, 46) deduced a value of 5 for the Taylor factor in titanium from a comparison of the critical resolved shear stress for prism slip in single crystals with σ_i from Hall-Petch plots of the effect of grain size \bar{d} on the flow stress σ of polycrystals, and from comparisons of the parameters associated with the deformation kinetics for polycrystals and for prism slip. An example of the agreement between σ_i and τ_{crss} for prism slip when a Taylor factor of 5 is used is given in Fig. 7. Also shown here is the agreement for the resolved shear stress at which $\{10\bar{1}0\} \frac{1}{2} \langle 11\bar{2}0 \rangle$ edge dislocations move at a velocity of 10^{-3} cm sec $^{-1}$ (30).

That the Taylor factor is relatively insensitive to the texture is indicated by the fact that those deformation kinetics parameters whose values include the Taylor factor (e.g., τ^* and the activation volume V^*) were found to be independent of grain size (and hence texture) in rod and wire (46). Furthermore, good agreement in flow stress and deformation kinetics parameters exists between polycrystalline wire or rod specimens (46) and sheet or plate specimens (47) of similar interstitial content.

c. Effects of Temperature, Interstitial Content and Grain Size on the Stress-Strain Behavior: Typical stress-strain curves over the temperature range of 4.2° to 1000°K for unalloyed titanium at a tensile strain rate $\dot{\epsilon} = 10^{-4}$ sec $^{-1}$ are given in Fig. 8. Serrations or

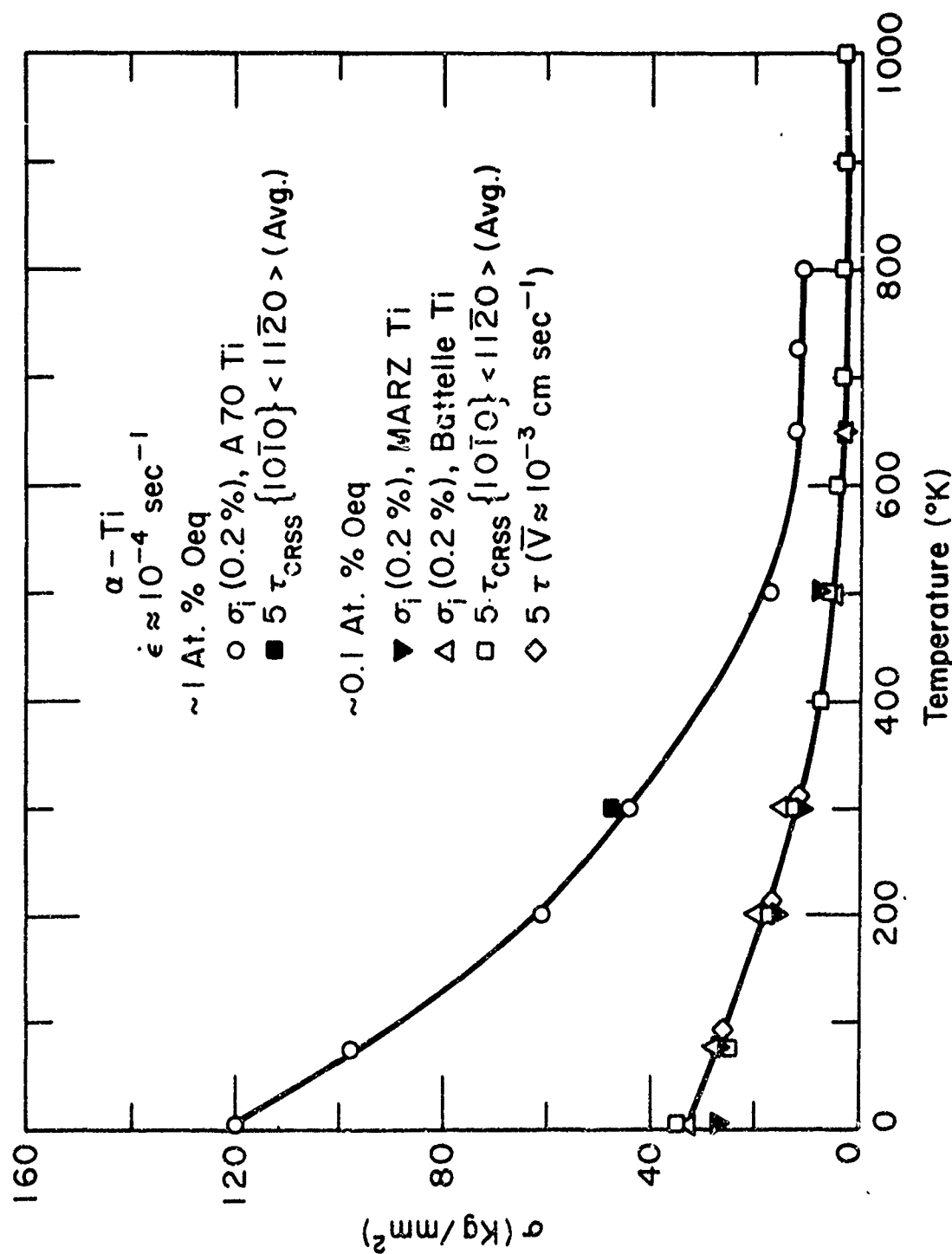


Fig. 7. Comparison of the effect of temperature on the flow stress of polycrystalline specimens with that for prism slip in single crystals and for the stress at which $\{10\bar{1}0\} \frac{1}{3} < 11\bar{2}0 >$ edge dislocations move at a velocity of $\sim 10^3 \text{ cm sec}^{-1}$. From Okazaki and Conrad (46)

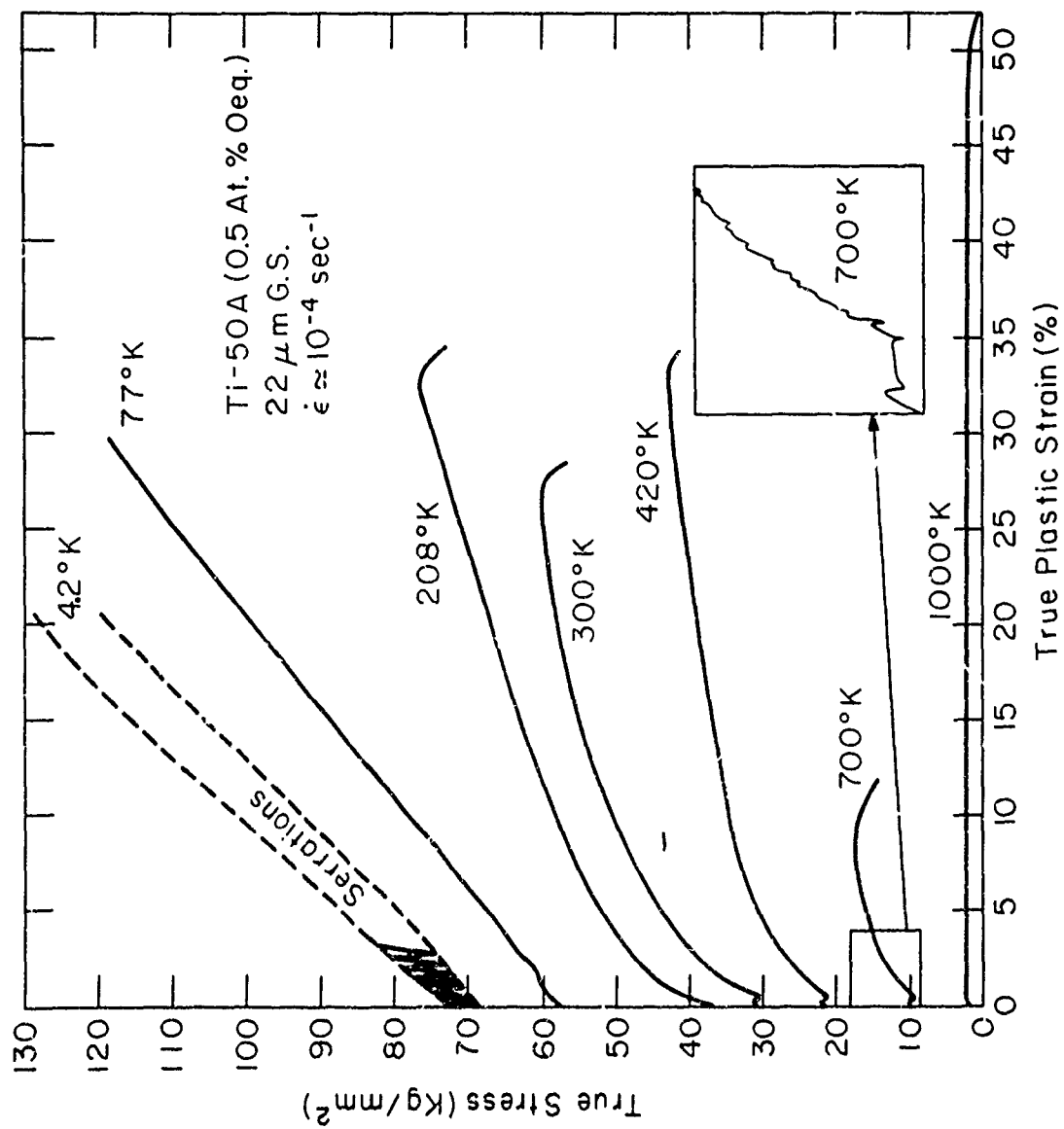


Fig 8. Stress-strain curves for unalloyed titanium (0.5 at.% Oeq) with 22 microns grain size as a function of temperature. Data from Refs. 10 and 40.

irregularities occur at 4.2°K and in the temperature range of 700° to 800°K. Those at 4.2°K appear to be due to twinning and adiabatic heating effects (48), while those in the range of 700° to 800°K to dynamic strain aging (49). The stress-strain curves are essentially flat in the temperature range of 900° to 1000°K, parabolic between 200° and 800°K and nearly linear at 4.2° and 77°K.

The effects of temperature, grain size and interstitial content on the 0.2% yield strength are illustrated in Fig. 9. The yield stress decreases continuously from 4.2° to about 600°K, remains relatively flat, or increases slightly, between 600° and 650°K and then decreases again above 700°K. The effect of an increase in the interstitial content is to increase significantly the temperature dependence of the yield stress. The effect of grain size at temperatures below about 700°K is to increase the yield stress a relatively constant amount independent of temperature and can be described by the Hall-Petch relation

$$\sigma = \sigma_i (T, \epsilon, \epsilon, C_i) + K (\mu) d^{-\frac{1}{2}} \quad (4)$$

with $K/\mu = 2 \times 10^{-4} \text{ mm}^{-\frac{1}{2}}$, relatively independent of interstitial content and temperature (46). As mentioned above, good agreement is obtained between σ_i for 0.2% strain and τ_{crss} for prism slip and in turn with the shear stress for $\{10\bar{1}0\} \frac{1}{3} \langle 11\bar{2}0 \rangle$ edge dislocation velocity of $\sim 10^{-3} \text{ cm sec}^{-1}$ for temperatures below about 700°K; see Fig. 7.

One means of describing strain hardening, which does not depend on a mathematical description of the stress-strain curve, is simply to take the difference in the flow stresses at two arbitrary values of the strain. This definition is used in Fig. 10, which is a plot of the flow stress at 5% strain minus that at 0.5% for commercial titanium plate ($\sim 0.5 \text{ at. \% Oeq}$) with 16 micron grain size (50). Superimposed on the general decrease in $\Delta\sigma$ which occurs with increase in temperature are three maxima located at approximately 250°K, 550°K and 750°K for a strain rate of $2.7 \times 10^{-4} \text{ sec}^{-1}$. The temperature of each maximum increases with increase in strain rate, yielding activation energies of 9, 32 and 57 Kcal/mole, respectively. It is difficult to relate these

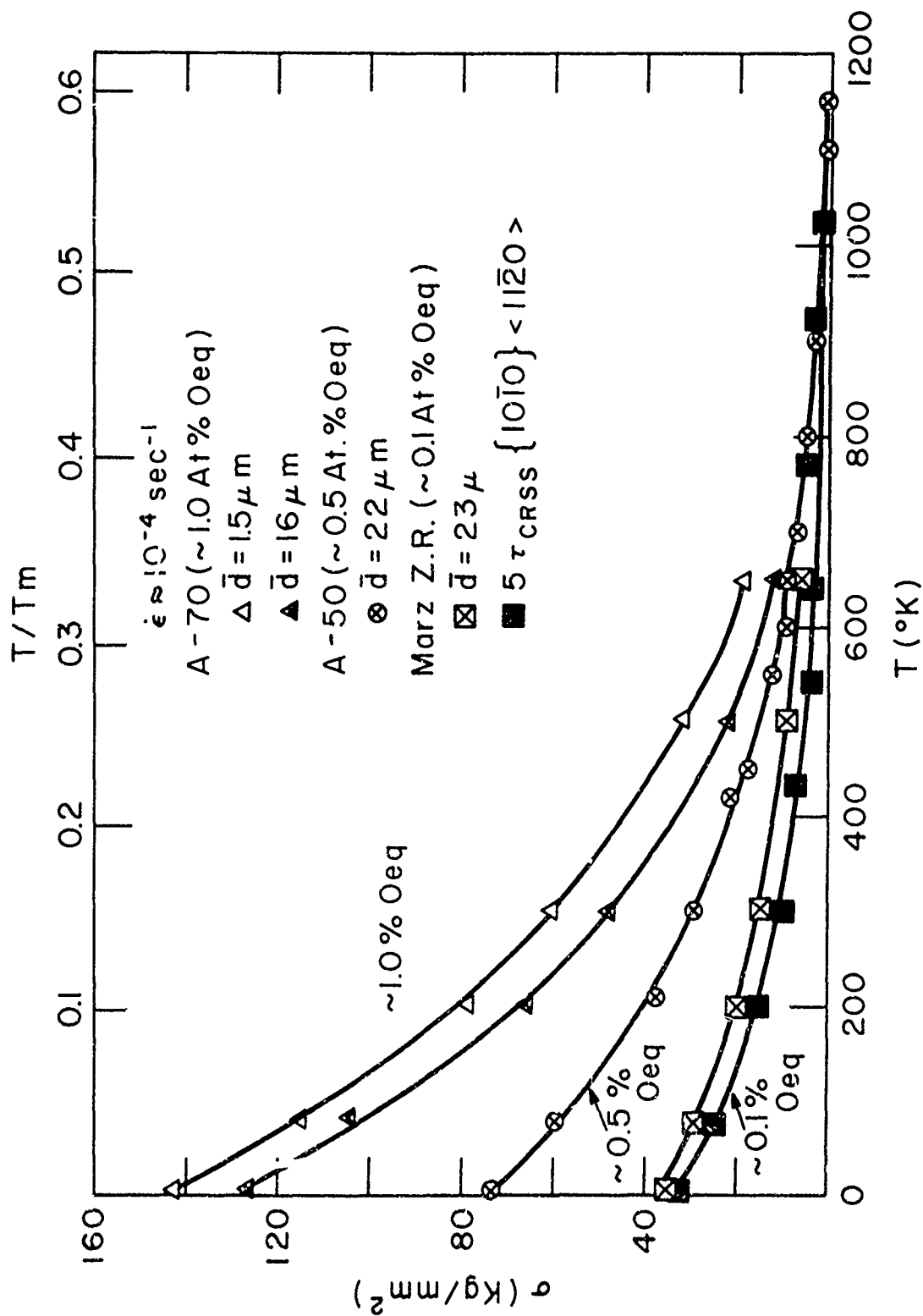


Fig. 9. Effects of temperature, grain size and interstitial content on the 0.2% yield stress. Data from Refs. 10, 27, 40 and 46.

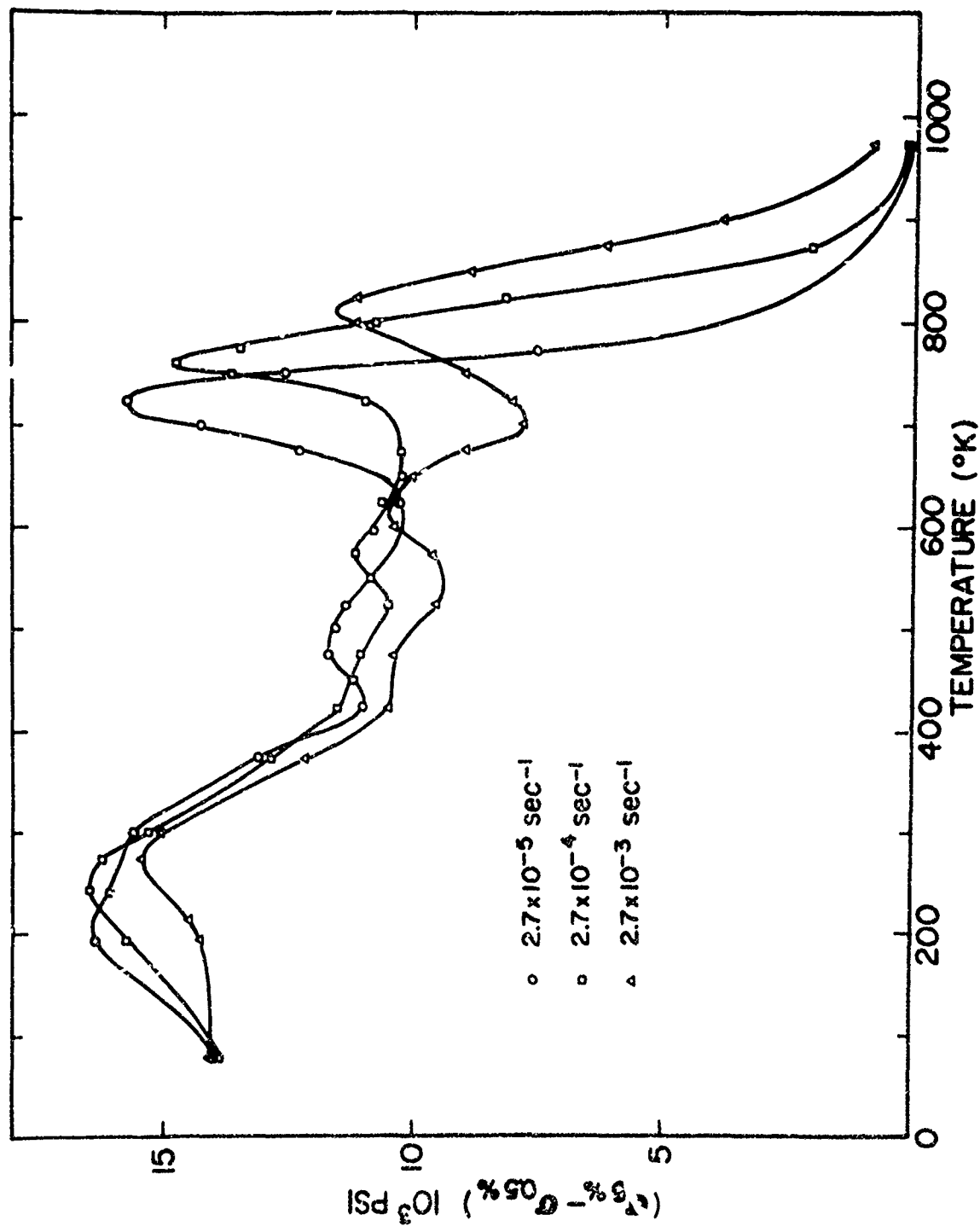


Fig. 10. Effect of temperature and strain rate on the strain hardening of titanium (0.5 at. % Oeq) with 16 micron grain size. From Santhanam and Reed-Hill (50).

values directly to activation energies for interstitial or substitutional solute diffusion in titanium because of the scatter in the diffusion data and the limited number of strain rates investigated in the mechanical tests. However, the relative magnitudes of the activation energies for strain hardening correspond roughly to those for diffusion of the interstitials H, C and O or N, respectively. Of further note in Fig. 10 is that the strain hardening decreases very rapidly for temperatures above about 800°K.

Okazaki and Conrad (46) investigated the strain hardening of annealed titanium wire as a function of interstitial content and grain size over the temperature range of 4.2° to 650°K. For zone refined material (~0.1 at.% Oeq) the strain hardening coefficient θ given by $\sigma_{.18} - \sigma_{.02} / 0.14$ divided by the modulus $\mu = C_{66}$ decreased rapidly with temperature between 4.2° and 200°K, only slightly between 200°K and then rapidly again above 500°K, relatively independent of grain size. In the case of commercial A-70 material (~1.0 at.% Oeq) there occurred a slight increase in θ/μ between 4.2° and 300°K and thereafter a slight decrease, again independent of grain size. At 4.2° and 77°K the strain hardening for the zone refined material was greater than that for the A-70 while at higher temperatures the reverse was true. The values of θ/μ were between 7.2×10^{-2} and 1.5×10^{-3} for the temperature, purity and grain size ranges considered.

Wasilewski (51) and Conrad and coworkers (46, 52-54) found that the stress-strain curves in titanium could be approximated by the relation

$$\sigma \approx \sigma^0(T, \bar{\epsilon}, \bar{d}, C_i) + h(\mu, T, \bar{\epsilon}, \bar{d}, C_i) \epsilon^{\frac{1}{2}} \quad (5)$$

σ^0 corresponded closely to the value of the proportional limit and h/μ decreased with temperature from values of the order of 10^{-2} at 77°K to near zero at 800°K.

The maxima in the strain hardening versus temperature curves of Fig. 10 suggest the occurrence of dynamic strain aging (49,50). Other evidence for dynamic strain aging in titanium includes: (a) serrations

in the stress-strain curves (Portevin-Le Chatelier effect) at 725° to 925°K (10, 52, 55), (b) a rise in the flow stress versus temperature curve at 675° to 750°K (47) and (c) a maximum in the creep strength in the vicinity of 475°K (56). Static strain aging in titanium has been observed by Rosi and Perkins (55) after heating in the temperature range of 473° to 673°K. Also, Kiessel and Sinott (56) found that the maximum creep resistance at room temperature occurred for cold-worked material aged for 100 hours at 477°K, compared to aging at lower or higher temperatures. Thus, there is little doubt that both static and dynamic strain aging occur in titanium, being most pronounced in the temperature range of 650° to 800°K ($0.3 - 0.4T_m$) at normal testing rates. However, the solutes (presumably interstitials) which are responsible for the various phenomena have not yet been clearly defined.

d. Deformation Kinetics at Low Temperatures ($T < 0.3T_m$): The results presented in Fig. 9 indicate that the flow stress σ in polycrystals, similar to single crystals, can be separated into a thermal component σ^* and an athermal component σ_μ . Work by Conrad and coworkers (46, 53, 54, 57, 58) has shown that

$$\sigma \approx \sigma^* (T, \dot{\epsilon}, C_i) + \sigma_\mu (\mu, \epsilon, \bar{d}, C_i, C_s) \quad (6)$$

where T is the temperature, $\dot{\epsilon}$ the tensile strain rate, C_i the interstitial solute content expressed as an oxygen equivalent, μ the modulus, ϵ the tensile strain, \bar{d} the average grain size and C_s the substitutional solute content. To be noted is that C_i affects both σ^* and σ_μ while ϵ , \bar{d} and C_s primarily influence σ_μ . σ^* was found to decrease in a linear fashion with the square root of the temperature and was proportional to the square root of the interstitial solute content. Using a Taylor factor of 5 there occurred good agreement between σ^* for polycrystals and τ^* for prism slip. Hence in the discussion to follow it will be assumed that $\tau = 1/5 \sigma$ and $\dot{\gamma} = 5\dot{\epsilon}$.

Plots of τ^* at 4.2°K and 300°K versus the square root of the interstitial content are presented in Fig. 11. The results indicate

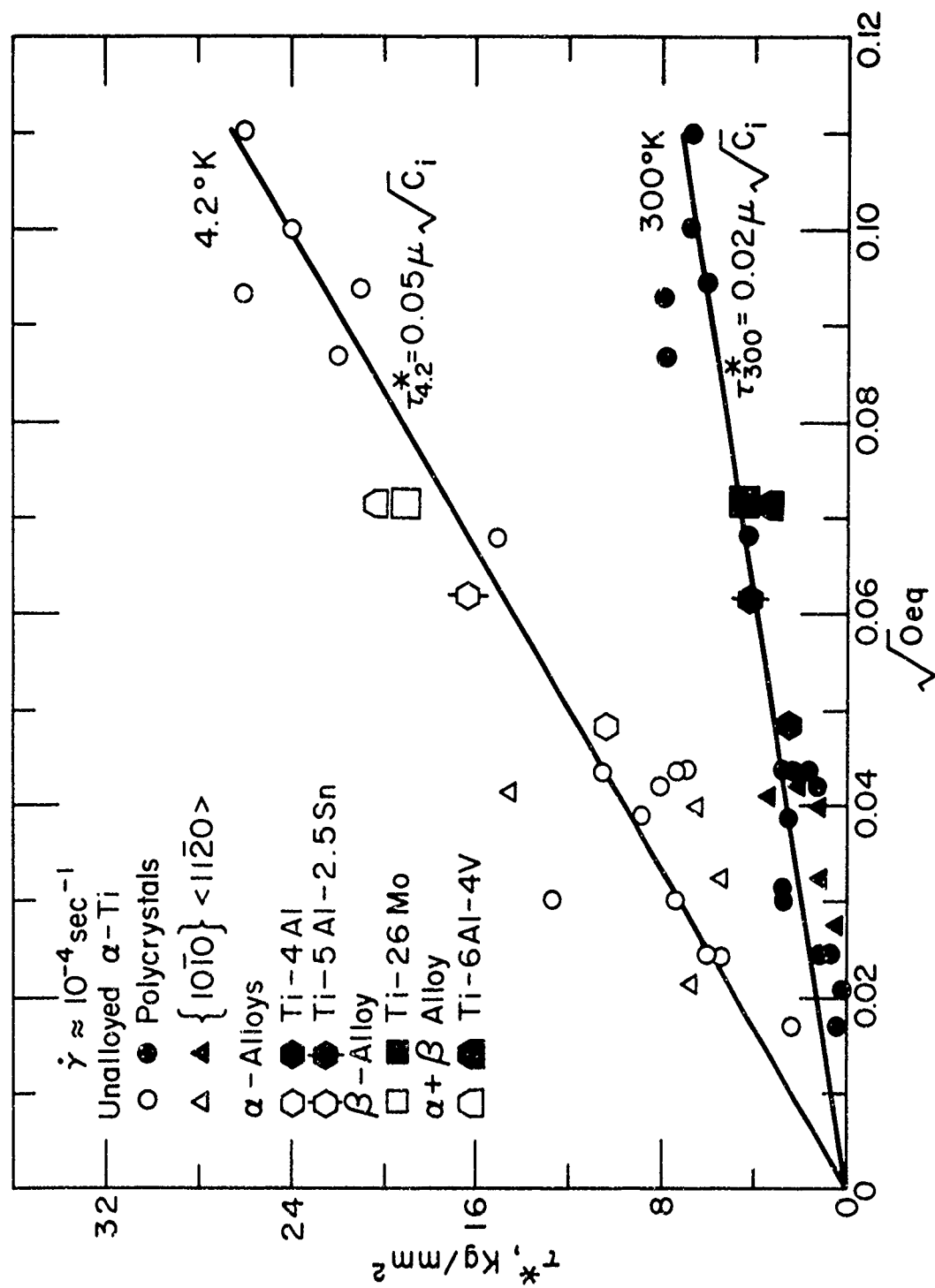


Fig. 11. τ^* at 4.2°K and 300°K versus the square root of the interstitial solute content for unalloyed titanium and some titanium alloys. Data from Refs. 27, 46, 58-61.

that τ^* is proportional to $C_i^{\frac{1}{2}}$ and that the proportionality constant decreases with temperature but is independent of the alloy content, crystal structure and whether the material is single-phase or two-phase. The value of τ_0^* is given by

$$\tau_0^* = 0.06 \mu_0 C_i^{\frac{1}{2}} \quad (7)$$

where μ_0 is C_{ss} extrapolated to 0°K . In Fleischer's (62) terminology this is a case of "rapid hardening".

A plot of the activation enthalpy H derived from constant strain rate type tests in the usual manner (32) versus the temperature is presented in Fig. 12. Good agreement occurs between prism slip in single crystals and plastic flow in unalloyed polycrystalline specimens and in polycrystalline alloys of the α (CPH) structure, the β (BCC) structure and $\alpha + \beta$ structures, independent of interstitial content over the range of 0.1 at.% to 1.0 at.% Oeq. The value of the activation energy at T_0^1 (510°K) is 1.24 eV ($0.29 \mu b^3$), that at T_0 (600°K) is 1.46 eV and the slope yields $v \approx 10 \times 10^8 \text{ sec}^{-1}$. Values of H obtained from stress relaxation test (57, 63) and from creep tests (64) are in good accord with those in Fig. 12 derived from constant strain rate tests.

The results of Figs. 11 and 12 indicate that overcoming of interstitial solute obstacles is the rate controlling mechanism during the low temperature deformation of titanium and titanium alloys of both the CPH and BCC structures. In the case of unalloyed α -titanium, the good agreement between the results on polycrystals and those for prism slip in single crystals and the stress for the motion of edge dislocations on the prism plane indicates that the deformation kinetics reflect the motion of individual dislocations on the prism plane. It is presumed that this also holds for the α -alloys, although this still needs to be confirmed. The fact that similar values of τ^* and the thermal activation parameters are obtained for the all- β Ti-26Mo alloy suggests that the strong interaction between dislocations and interstitials in titanium is relatively independent of crystal structure.

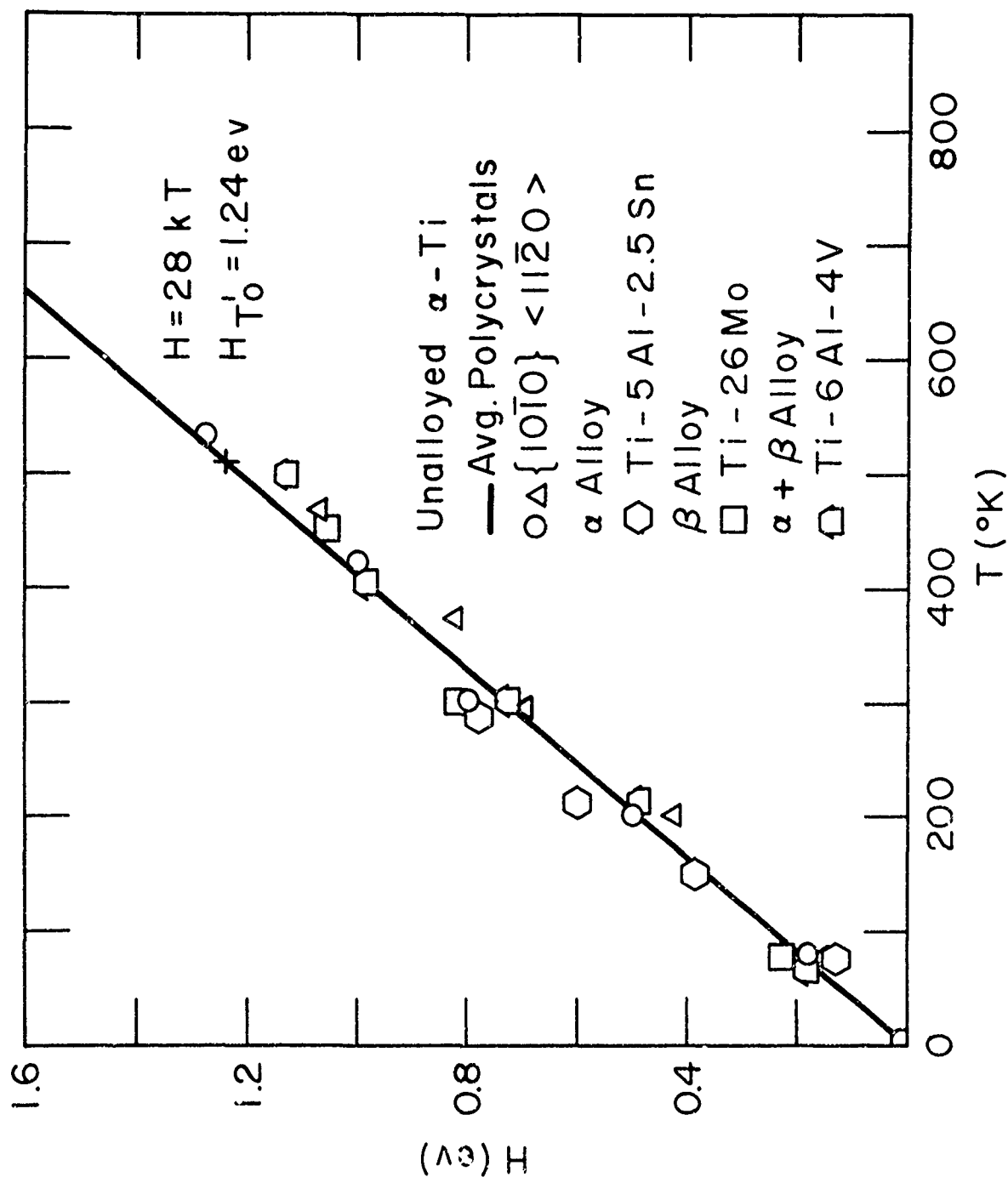


Fig. 12. Activation enthalpy versus temperature for the deformation of unalloyed titanium and some alloys. Data from Refs. 27, 46, 58, 60, 61.

Assuming that overcoming interstitial solute atoms is rate controlling, a force-activation distance curve was derived (27, 46) from data on unalloyed titanium for the case of a random distribution of obstacles (65) and taking into consideration dislocation line flexibility (66); see Fig. 13. The approximately triangular shape of the F - d^* curve is in accord with the experimentally observed dependence of τ^* on $T^{\frac{1}{2}}$. Moreover, the area under the F - d^* curve between $d^*/b = 0$ and $d^*/b = 1.5$ yields $H = 1.3$ eV in good accord with the value of $H_{T_0}^1$. Of significance is that a rapid rise in the force first occurs at $d^* \approx 1.5b$. The maximum force $F_0 = 82 \times 10^{-6}$ dynes ($0.21 \mu_0 b^2$). The detailed nature of the interaction between the moving dislocations and the interstitial solutes which leads to the F - d^* curve of Fig. 13 is, however, still not clear (67).

e. Athermal Component at Low Temperatures ($T < 0.3T_m$): It has been shown (54, 68-72) that there is reasonably good agreement in the value of the athermal component of the flow stress in titanium determined by a number of methods which include: (a) back-extrapolation of the flow stress at high temperatures, (b) the fully relaxed stress, (c) incremental unloading, (d) analysis of the stress relaxation curve, (e) single strain rate cycling, (f) double strain rate cycling, (g) the grain size method, (h) dislocation density versus flow stress and (i) measurements of the dislocation curvature.

Conrad and coworkers (54, 68, 69, 73) have established that the effect of grain size on the athermal component of the flow stress in unalloyed titanium is principally through its effect on the dislocation density ρ at a given strain and that flow stress increased in a linear fashion with $\rho^{\frac{1}{2}}$; see Fig. 14. Moreover, the effect of interstitial solute content on σ_μ was also primarily through the effect on the dislocation density. The dislocation density measurements on unalloyed titanium yield

$$\tau = \tau^*(T, \dot{\gamma}, C_i) + 0.5 \mu b \{ \rho(\gamma, \bar{d}, C_i) \}^{\frac{1}{2}} \quad (8)$$

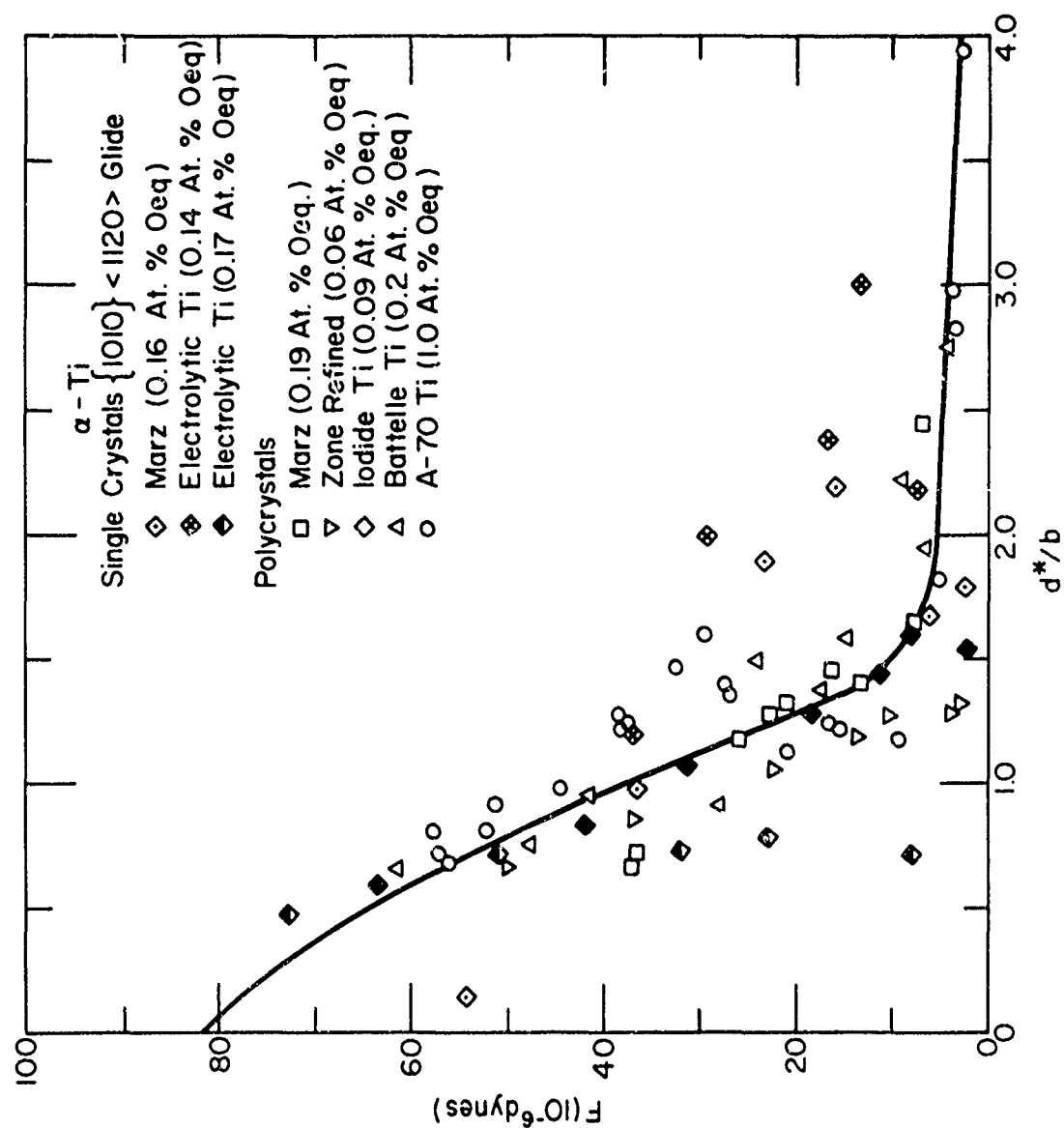


Fig. 13. Force-activation distance curve for the deformation of unalloyed titanium at low temperatures.
From Okazaki and Conrad (46).

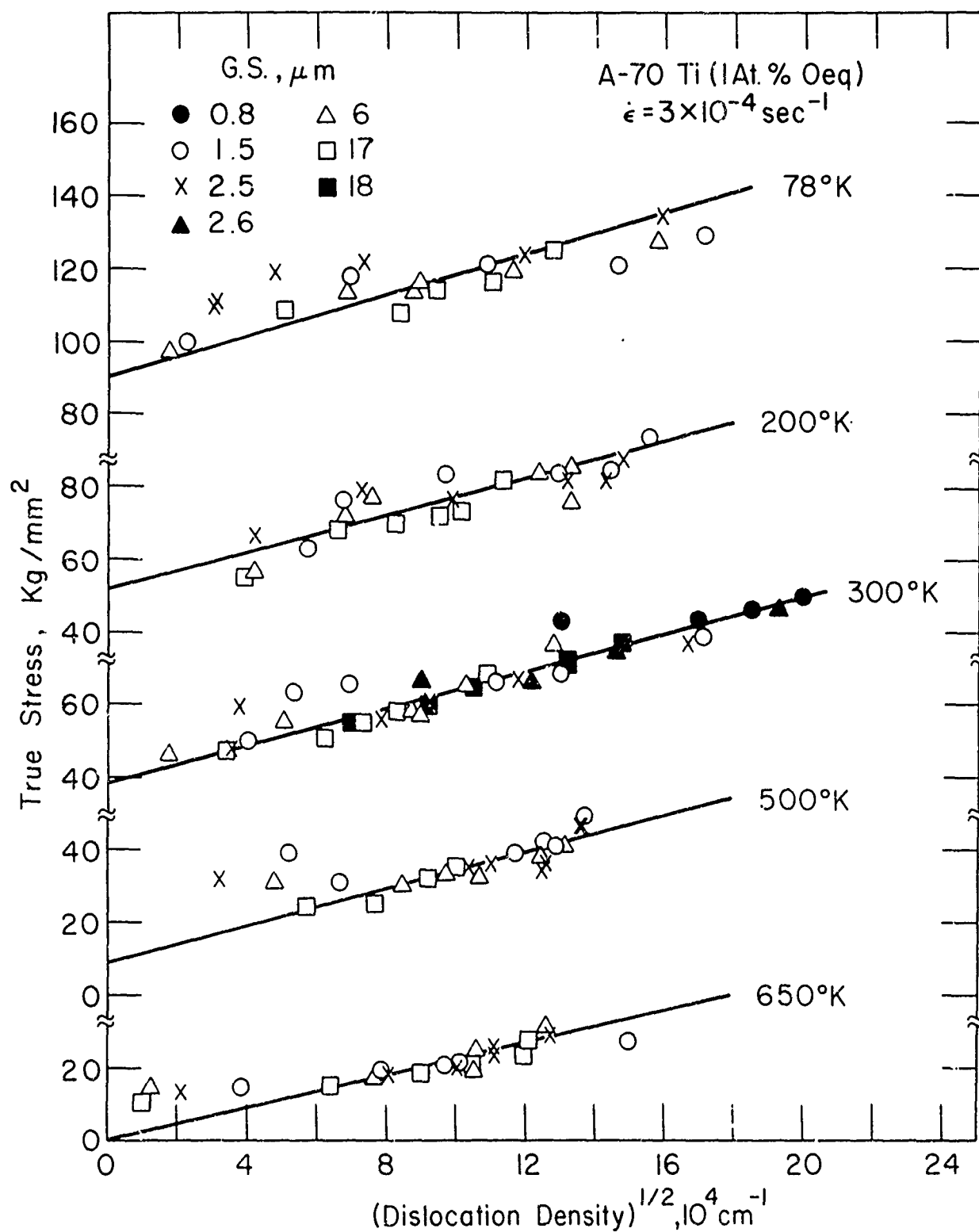


Fig. 14. Flow stress versus the square root of the dislocation density in A-70 titanium (1.0 at.% Oeq) as a function of grain size and temperature. From Conrad et al. (54).

Thus, the effects of temperature, interstitial content and grain size on strain hardening are through the accumulation of dislocations as a function of strain, i.e. through the multiplication and annihilation of dislocations. In fact, values of the strain hardening coefficient h and the Hall-Petch constant K derived from dislocation measurements are in good accord with those determined from stress-strain curves (54, 68, 73). Further interpretation of the effects of temperature, grain size and interstitial content on strain hardening in unalloyed titanium must await the development of a more detailed model for dislocation multiplication. The rapid increase in strain hardening at very low temperatures in the higher purity materials is probably due to twinning.

The value of 0.5 for the coefficient relating the flow stress to $\rho^{1/2}$ is in accord with that for most metals and with most strain hardening mechanisms (74) and hence does not permit an identification of the specific dislocation mechanism responsible for strain hardening in titanium.

Considering the linear decrease in τ^* with $T^{1/2}$ Eqn. 8 can be expanded to

$$\tau \approx \left\{ 27 - 14.7 T^{1/2} \log_{10} \left(\frac{5 \times 10^8}{\dot{\gamma} (\text{sec}^{-1})} \right) \right\} C_i^{1/2} + 0.5 \mu b \rho^{1/2} \quad (\text{Kg/mm}^2) \quad (9)$$

As pointed out above, the effect of substitutional solutes on the flow stress of titanium at low temperatures is primarily through the athermal component of the flow stress. Fig. 15 shows that the increase in tensile strength due to substitutional solutes which are α -stabilizers can be considered to be proportional to the square root of the atomic fraction of the solute content. Gegel and coworkers (75) have shown that the slopes of the straight lines of Fig. 15 are proportional to the interaction parameter given by the sum of the square root of the absolute magnitude of the individual interaction coefficients Δ as defined by Fowler and Guggenheim (76). This proportionality is depicted in Fig. 16, where the individual interaction coefficients are expressed in electron volts per atom. The interaction parameter is similar to the Pauling electronegativity difference, which has been used by Kubaschewski

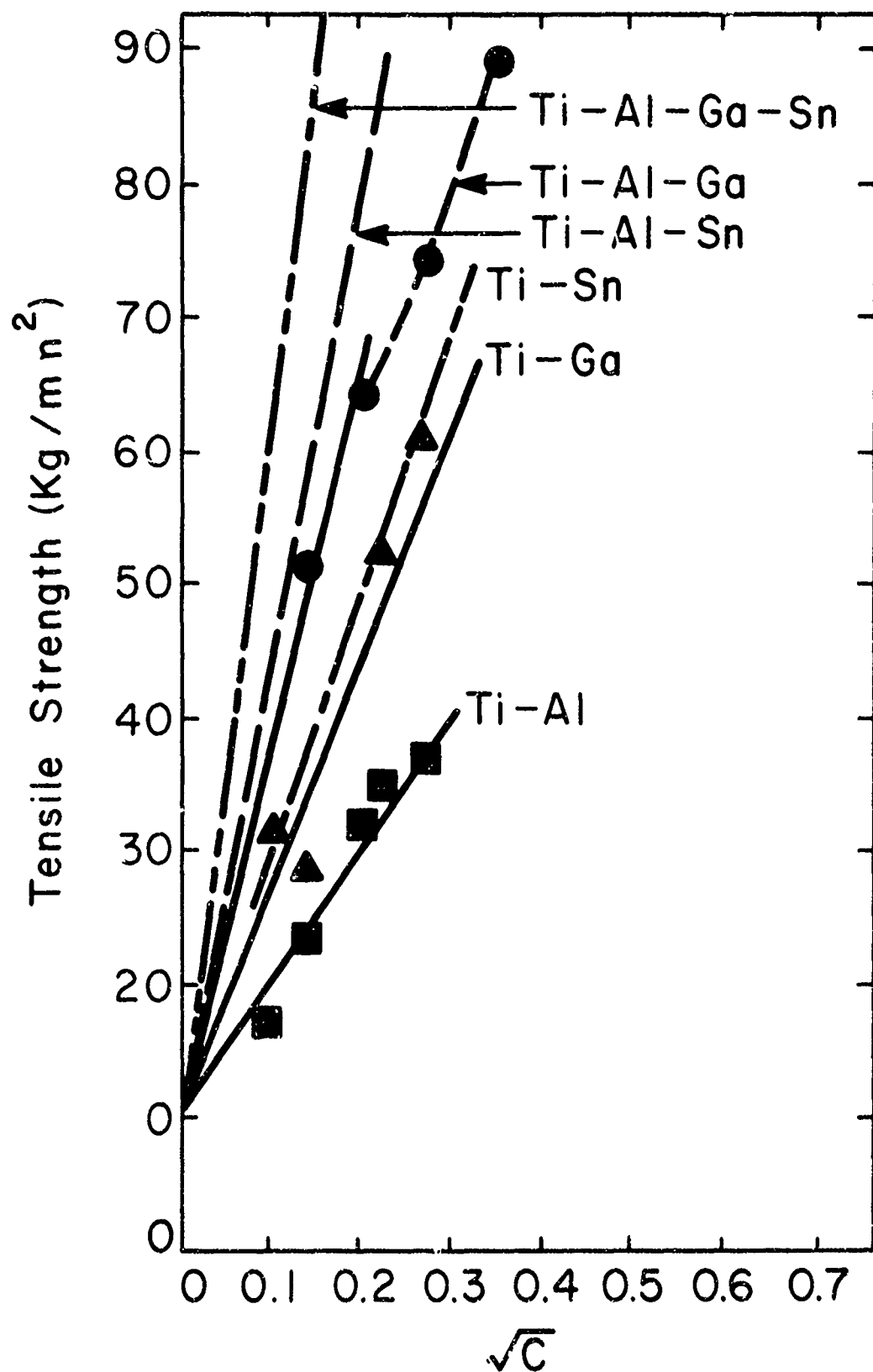


Fig. 15. Tensile strength at room temperature versus square root of the atomic fraction of a α -stabilizing solutes. From Gegel (75).

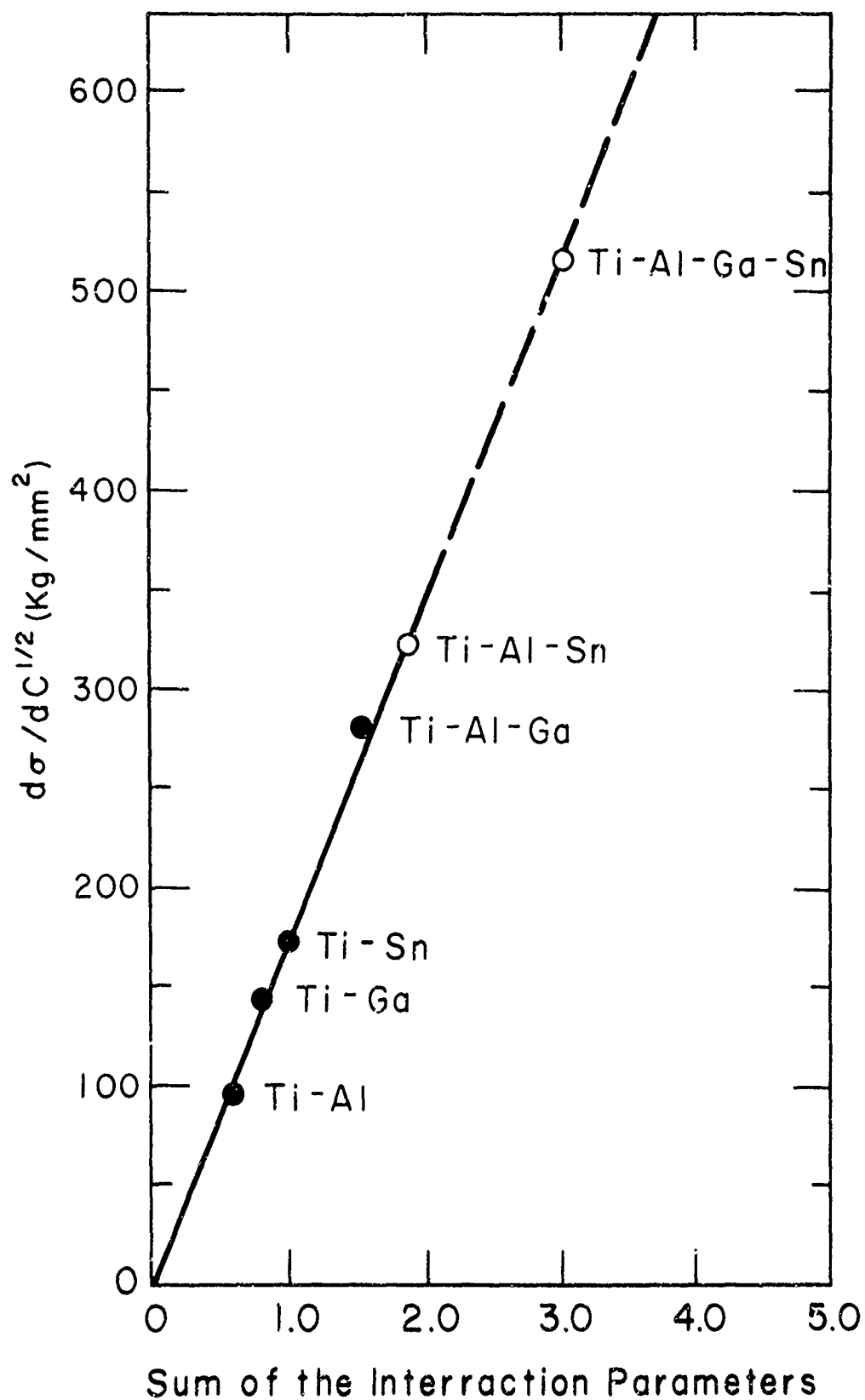


Fig. 16. $d\sigma/dc^{1/2}$ versus the interaction parameter defined as the sum of the square roots of the absolute values of the individual interaction coefficients expressed in eV per atom. From Gegel (75).

and Sloman (77) in treating bonding mechanisms in intermetallic compounds. Of considerable importance regarding the data of Figs. 15 and 16 is that the strengthening results from the sum of all individual atom-atom interactions, including those between the individual solutes, as well as between titanium and each solute.

Considering the results of Figs. 15 and 16, we can expand Eqns. 6 and 8 for the α -stabilizing solutes to

$$\tau = \tau^* (T, \dot{\gamma}, C_i) + 0.5\mu b\rho^{\frac{1}{2}} + 34.1 I C_{\alpha}^{\frac{1}{2}} \text{ (Kg/mm}^2\text{)} \quad (10)$$

where I is the interaction parameter defined above and C_{α} is the concentration of α -stabilizing solutes.

An explanation for the effect of substitutional solutes on the strength of titanium in terms of dislocation-solute interactions is not yet available. However, Collings and coworkers (78) have developed a rationalization for the strengthening of α and β stabilizing solutes in terms of certain electronic factors. Their interpretation is the following: The significant solid solution strengthening of α -stabilizing solutes is due to the tendency for directional (partially covalent) bond formation by these solutes. The β -stabilizing solutes (transition elements) increase the conduction electron density and thereby there does not occur any tendency for directional bonding. Hence, the strengthening by the β -stabilizers which is largely due to d-electron bonding is considerably less than that of the α -stabilizers. Some correlation of the mechanical properties in the former alloys is obtained through the average group number or the electron-to-atom ratio.

f. Role of Twinning: The nature and role of twinning during the low temperature deformation of unalloyed polycrystalline titanium was investigated by Conrad and coworkers (40, 46, 54). Employing electron transmission microscopy they found that the tendency for twinning in wires deformed to a maximum strain of 10% increased with increase in purity, strain, grain size and temperature. Zone refined material (~ 0.1 at.% Oeq) exhibited twinning for all grain sizes (1 to 23 microns)

at 78° and 200°K. At 300°K twinning was only seen in specimens with grain sizes in the range of 5 to 23 microns. No twins were observed for any grain size of this material at 500° and 650°K. Commercial A-70 material (1.0 at.% Oeq) exhibited some twinning for all grain sizes at 78°K but only the largest grain size (17 microns) at 200°K. No twins were observed in this material for any grain size (1.5 to 17 microns) at 300°K and above. When twinning occurred, the thermal component of the flow stress σ^* tended to be less than that in material where no twinning was evident, and in turn below that predicted from the single crystal results using a Taylor factor of 5. By correcting for the contribution of twinning to the total strain, good agreement in σ^* was obtained between material exhibiting twins and that with no evidence of twins (40).

Reed-Hill and coworkers (79, 80) found that the volume fraction of twins in polycrystalline titanium wire and sheet was approximately proportional to the strain, with the proportionality constant decreasing with increase in temperature. Moreover, the amount of twinning increased with increase in purity. They attributed the linear stress-strain behavior at 78°K to the deformation twins and concluded that most of the temperature and strain dependence of the strain anisotropy in titanium sheet can be accounted for by twinning.

g. Deformation at High Temperatures ($T > 0.4T_m$): Weertman's (81) model for the high temperature deformation of metals based on dislocation climb leads to

$$\dot{\epsilon}_s = \frac{3\pi^2 \sigma^2 D}{2\sqrt{2}\mu^2 b^2} \sinh \left(\frac{\sqrt{3} \sigma^{2.5} b^{1.5}}{8\mu^{1.5} N^{\frac{1}{2}} kT} \right) \quad (11)$$

where $\dot{\epsilon}_s$ is the steady-state strain rate, σ is the applied tensile stress, μ the shear modulus and N the density of Frank-Read sources per cm^3 . At low stresses Eqn. 11 reduces to the power law relation

$$\dot{\epsilon}_s = \frac{3\sqrt{6} \pi^2 \sigma^{4.5} D}{2^{1.5} b^{\frac{1}{2}} N^{\frac{1}{2}} \mu^{3.5} kT} \quad (12)$$

Hence, at low stresses a plot of $\log \dot{\epsilon}_s kT/D\mu b$ versus $\log \sigma/\mu$ should yield a straight line of slope 4.5. Such a plot is given in Fig. 17 for the available data on the high temperature deformation of unalloyed α - and β -titanium. The values of D which give the good fit indicated in Fig. 17 are $55 \exp \{-60,000/RT\}$ for α -titanium and $55 \exp \{-55,000/RT\}$ for β -titanium. These values were chosen on the basis of the empirical correlation of the activation energy for diffusion with the melting temperature (82) and Zener's (83) theory for D_0 . A slightly better fit was obtained using $D = 1.0 \exp \{-56,500/RT\}$ for α -titanium and $D = 1.0 \exp \{-50,000/RT\}$ for β -titanium. These latter values are in reasonable agreement with the "best" self-diffusion data for titanium, Table II.

The correlation of Fig. 17 yields $N = 6.5 \times 10^{13} \text{ cm}^{-3}$ and $\rho = \{(1.9 N^{1/2})^{4/3}\} = 3.9 \times 10^9 \text{ cm}^{-2}$. Using the second set of values for D gives $N = 2.8 \times 10^{12} \text{ cm}^{-3}$ and $\rho = 4.7 \times 10^8 \text{ cm}^{-2}$. Both sets of values for N and ρ are reasonable; however, the lower values are in better agreement with the dislocation densities measured in metals deformed at high temperatures (87). It is thus concluded that the high temperature deformation of α - and β -titanium is controlled by dislocation climb.

The creep of binary Ti-Mo alloys has been studied by Collings et al (4). These investigators concluded that above 1073°K creep was glide controlled, i.e. dislocation glide limited by the drag of Cottrell atmospheres. The activation energies (28-44 Kcal/mole) obtained for creep were in the range of values reported for the diffusion of Mo in binary Ti-Mo alloys. However, one may question the creep activation energies, since there existed considerable curvature in the plots of \log creep rate versus $1/T$. Also, there is some question regarding the activation energy for the diffusion of Mo in Ti-Mo alloys (88).

Fracture

1. Unidirectional Stressing: Tension

a. Fracture Modes at Low Temperatures: In studies of fracture

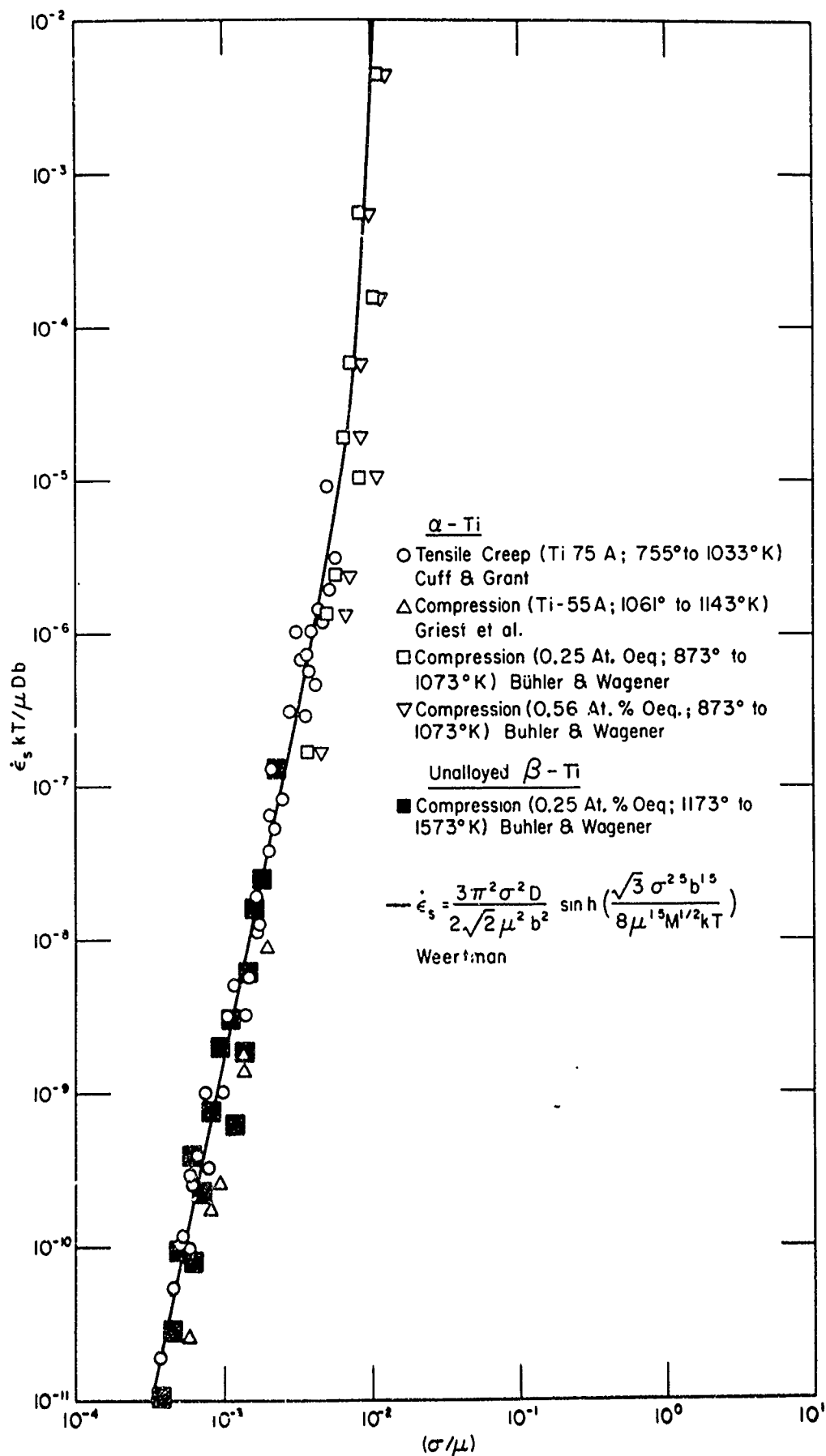


Fig. 17. Log $\dot{\epsilon}_s kT/D_0 b$ versus log σ/μ for the deformation of α - and β -titanium at high temperatures. Data from Refs. 84 - 86.

in large grain size titanium of commercial purity (~ 1.0 at.% Oeq), Amateau et al. (89, 90) found that at low temperatures cracks developed at the interface between second-order twins (in primary $\{11\bar{2}2\}$ twins) and the matrix or first-order twins. Further, they found a correlation between ductility and the number of grains containing second-order twins. At temperatures above about 200°K the fracture mode was normal shear type.

b. Effects of Temperature, Grain Size and Solute Content on the Fracture Behavior at Low Temperatures ($T < 0.3T_m$): The effects of temperature, solute content and grain size on the fracture stress σ_F (= load at fracture/cross section area at fracture) is illustrated in Fig. 18. The fracture stress, similar to the flow stress, can be considered to consist of thermal and athermal components, i.e.

$$\sigma_F = \sigma_F^*(T, \bar{z}, C_i) + \sigma_{\mu_F}(\mu, \bar{d}, C_s, C_s) \quad (13)$$

The temperature dependence of σ_F^* for the A-70 (1.0 at.% Oeq) material is only slightly higher than that of the flow stress for this material. The difference is essentially eliminated if the Bridgman's (92) correction for necking is applied to the fracture stress. However, there does not appear to be as strong an effect of interstitial content on the fracture stress as occurs for the flow stress. The reason for this is not clear.

The effect of grain size on the fracture stress (40, 91, 93) can be considered to obey the Hall-Petch relation yielding values of $\sigma_i = 80$ to 115 Kg/mm^2 and $K_F = 1.0 - 1.4 \text{ Kg/mm}^{\frac{3}{2}}$ at room temperature, relatively independent of interstitial solute content. The value of K_F is about twice that of K for plastic flow. From the curves in the upper part of Fig. 18 it is seen that the effect of the substitutional solute Mo on the fracture stress appears to be mainly through the athermal component.

The effects of the interstitials C, N and O on the total elongation at fracture at 300°K are presented in Fig. 19. In each case the elongation decreases with increase in interstitial content, the rate

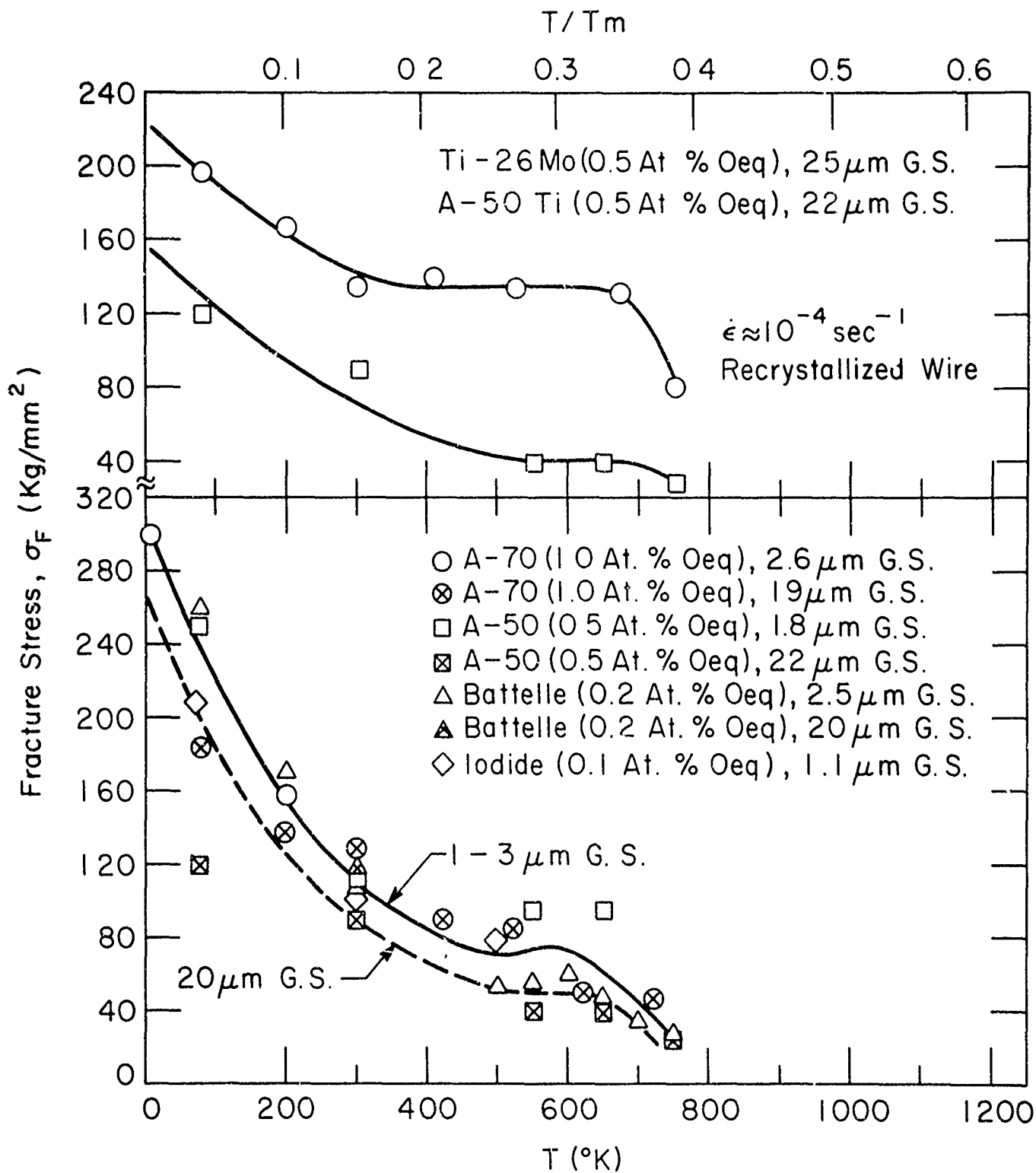


Fig. 18. Effects of temperature, solute content and grain size on the fracture stress of titanium. Data from Refs. 40, 58, 91.

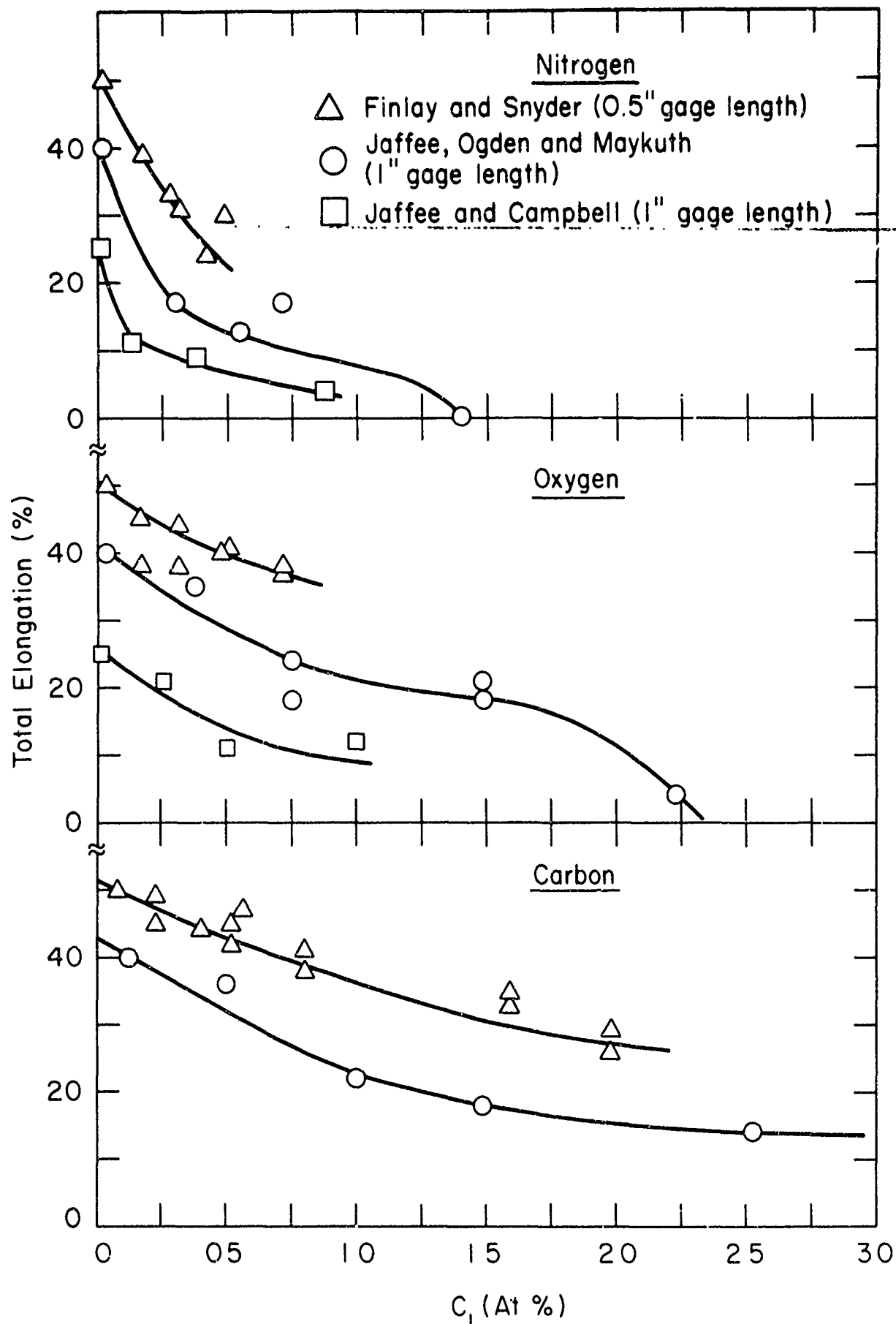


Fig. 19. Effects of the interstitials, C, O and N on the total elongation at fracture at 300°K. Data from Ref. 94-96.

being greatest for the lowest concentrations. The rate of decrease in elongation with interstitial content increases in the order C, O, N, which is the same order as their effect on the flow stress (28). The total elongation is relatively independent of grain size (91).

The effects of temperature and strain rate on the total elongation are presented in Fig. 20. To be noted is that a minimum in the elongation occurs in the vicinity of 750°K for a strain rate of $2.7 \times 10^{-4} \text{ sec}^{-1}$, the temperature of which increases with increase in strain rate. The activation energy derived from the effect of strain rate on the temperature of this minimum is 48 Kcal/mole, in reasonable accord with the diffusion of Oh in titanium, Table II. The minimum in elongation thus appears to be related to the dynamic strain aging which occurs in this temperature range (49, 50).

The fracture mode in polycrystalline specimens at low temperatures is most generally of the cup-cone shear type.

c. Fracture at High Temperatures ($T > 0.4T_m$): Orr et al (97) have shown that the stress-rupture data for titanium correlated very well through the relation

$$\sigma_F = f(t_r \exp \{-60,000/RT\}) \quad (14)$$

where σ_F is the fracture stress and t_r is the time to rupture. The value of the activation energy for rupture is thus similar to that for creep and suggests that the same mechanism is controlling, namely the climb of dislocations.

2. Fatigue

Unalloyed titanium exhibits a well defined fatigue limit between 77° and 673°K, the level of which increases with interstitial content (Fig. 21) and with decrease in grain size and temperature (98-103). From Fig. 22 it is seen that the ratio of the fatigue limit to the yield stress at 300°K is approximately constant, relatively independent of interstitial content and grain size, suggesting that the high cycle fatigue strength is controlled by the same dislocation mechanisms as the

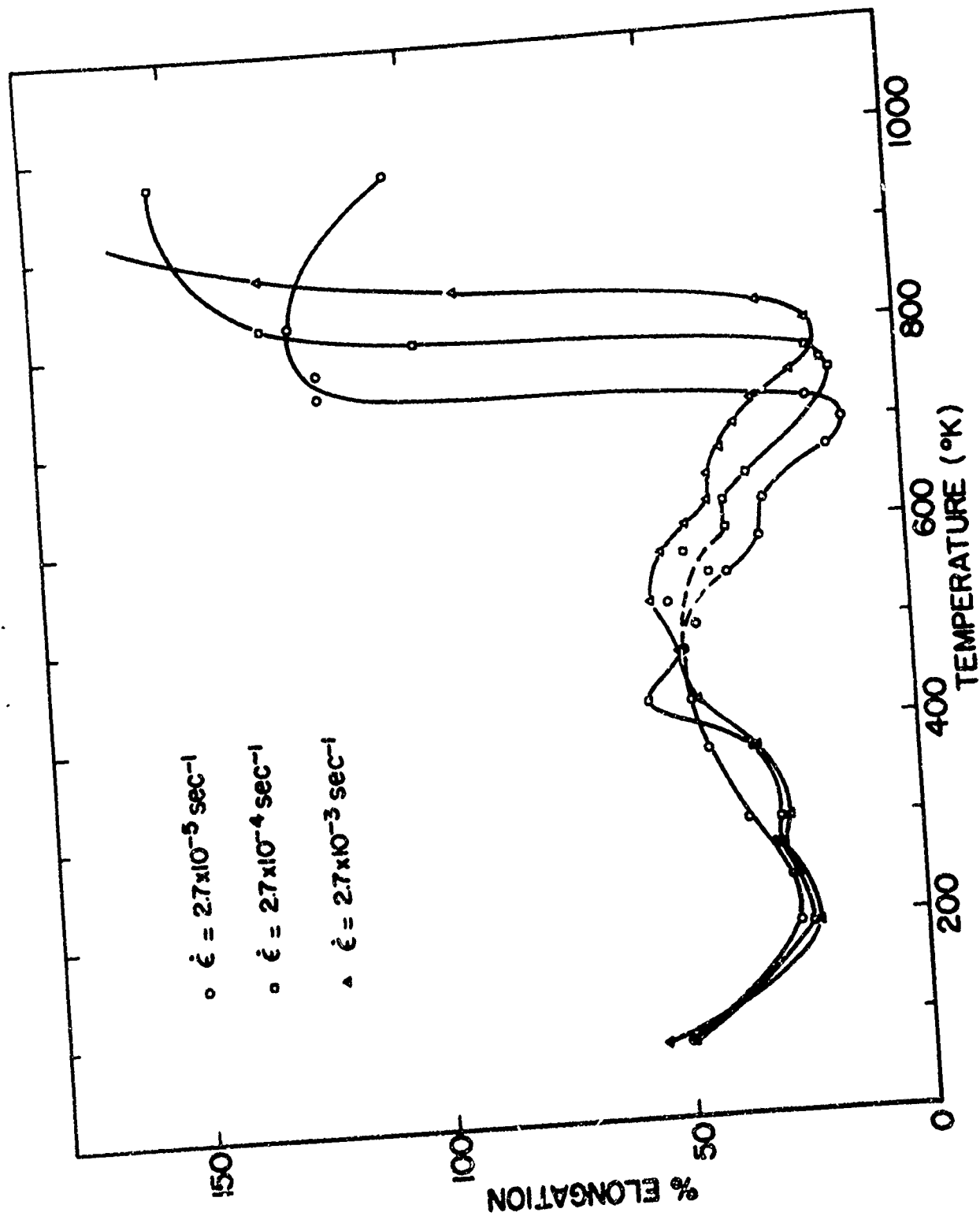


Fig. 20. Effects of temperature and strain rate on the total elongation at fracture in commercial purity titanium (~ 0.5 at. % Oeq) sheet of 16 micron grain size. From Santhanam and Reed-Hill (50).

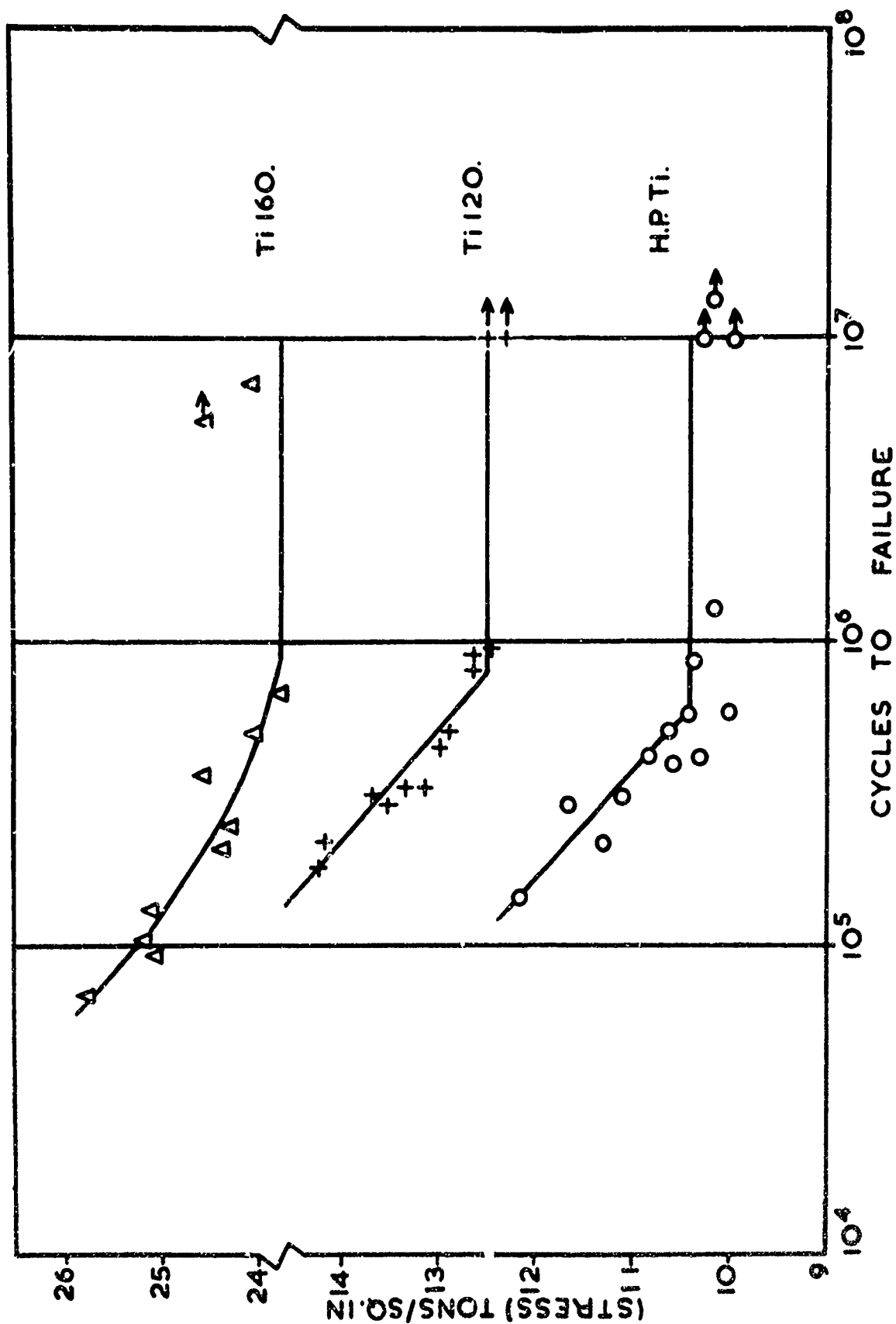


Fig. 21. Effect of interstitial content on S-N curves of unalloyed titanium with 32 micron grain size at 300°K. Interstitial contents in terms of Oeq are: Ti 160 (1.1at%), Ti 120 (0.4 at%) and H.P.Ti (0.3 at%). From Turner and Roberts (100).

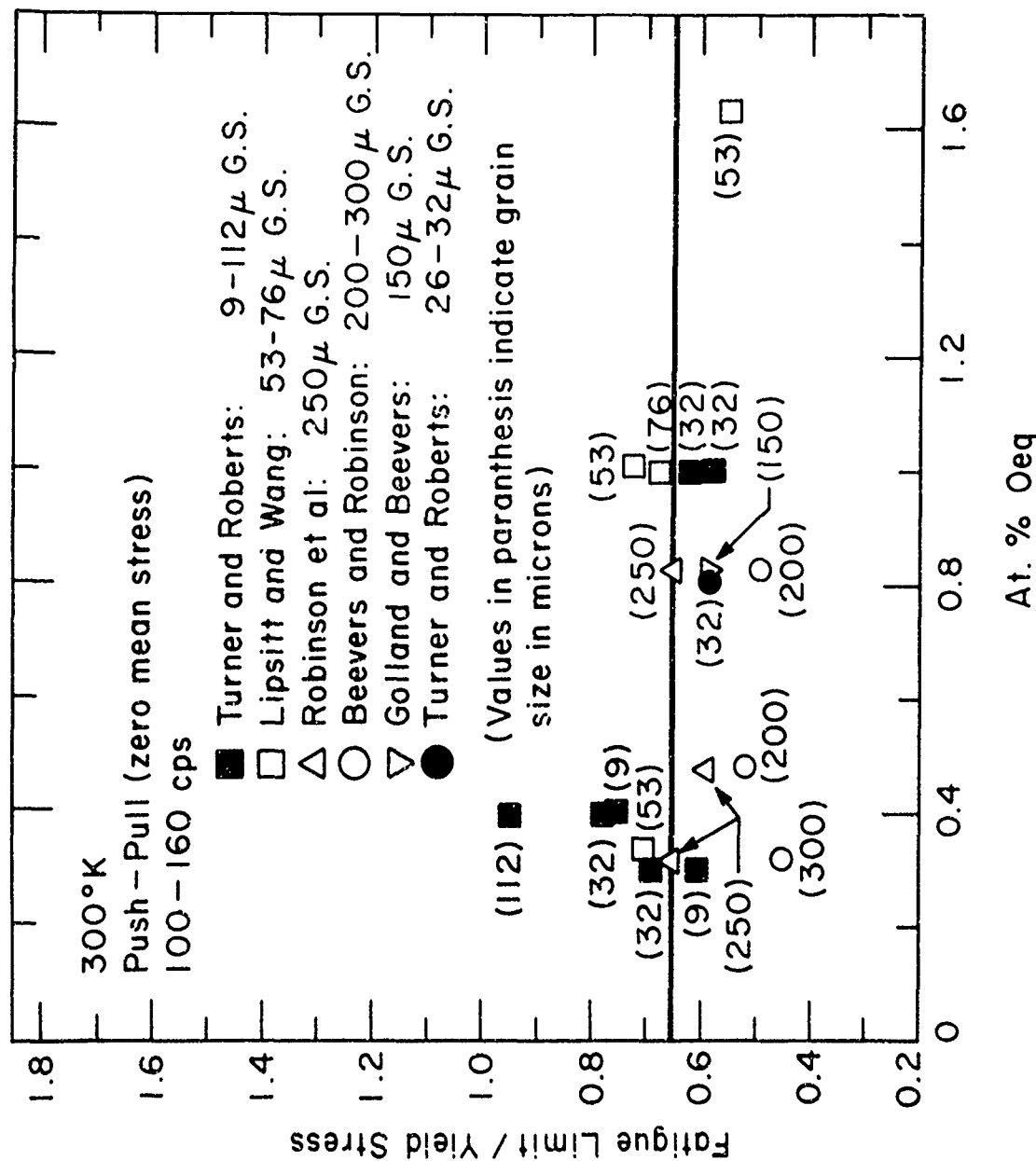


Fig. 22. Ratio of the fatigue limit to the yield stress in unalloyed titanium at 300°K as a function of interstitial content and grain size. Data from Refs. 98-104.

flow stress. This conclusion is further supported by the results presented in Fig. 23, which contains plots of the ratio of the stress to cause failure at 10^6 cycles to the yield stress and the ratio of the fatigue limit (F.L.) to the yield stress (Y.S.) as a function of temperature. These ratios are relatively independent of temperature below about 450°K, but go through a maximum at higher temperatures. The maximum is probably related to the strain aging which occurs in this temperature range.

The observation that the F.L./Y.S. ratio and the ratio of the stress to cause failure at 10^6 cycles/Y.S. remain relatively constant with decreasing temperature below 300°K is not in accord with the commonly held belief that the low temperature fatigue behavior of unalloyed titanium is controlled by twinning (101-107).

The fracture modes under cyclic deformation in coarse-grained α -Ti have been investigated by Golland and Beevers (102). They reported that in the temperature range of 77° to 195°K fatigue cracks were associated with $\{11\bar{2}1\}$ type twins, slip bands and grain boundaries. The fracture surfaces exhibited twin-assisted transgranular and intergranular fracture paths. In the range of 473° to 773°K the failure occurred as a consequence of the transgranular propagation of surface nucleated cracks; between 873°K and 973°K the fatigue fracture was intergranular; above 973°K the internal fatigue damage existed in the form of grain boundary cavities.

Acknowledgement

The authors wish to express their appreciation to Drs. H. Gegel and E. Collings for permission to use their results on substitutional alloy strengthening prior to publication. They also wish to acknowledge financial support for this investigation under contract AF33615-68-C-1052, Dr. H. Gegel technical monitor.

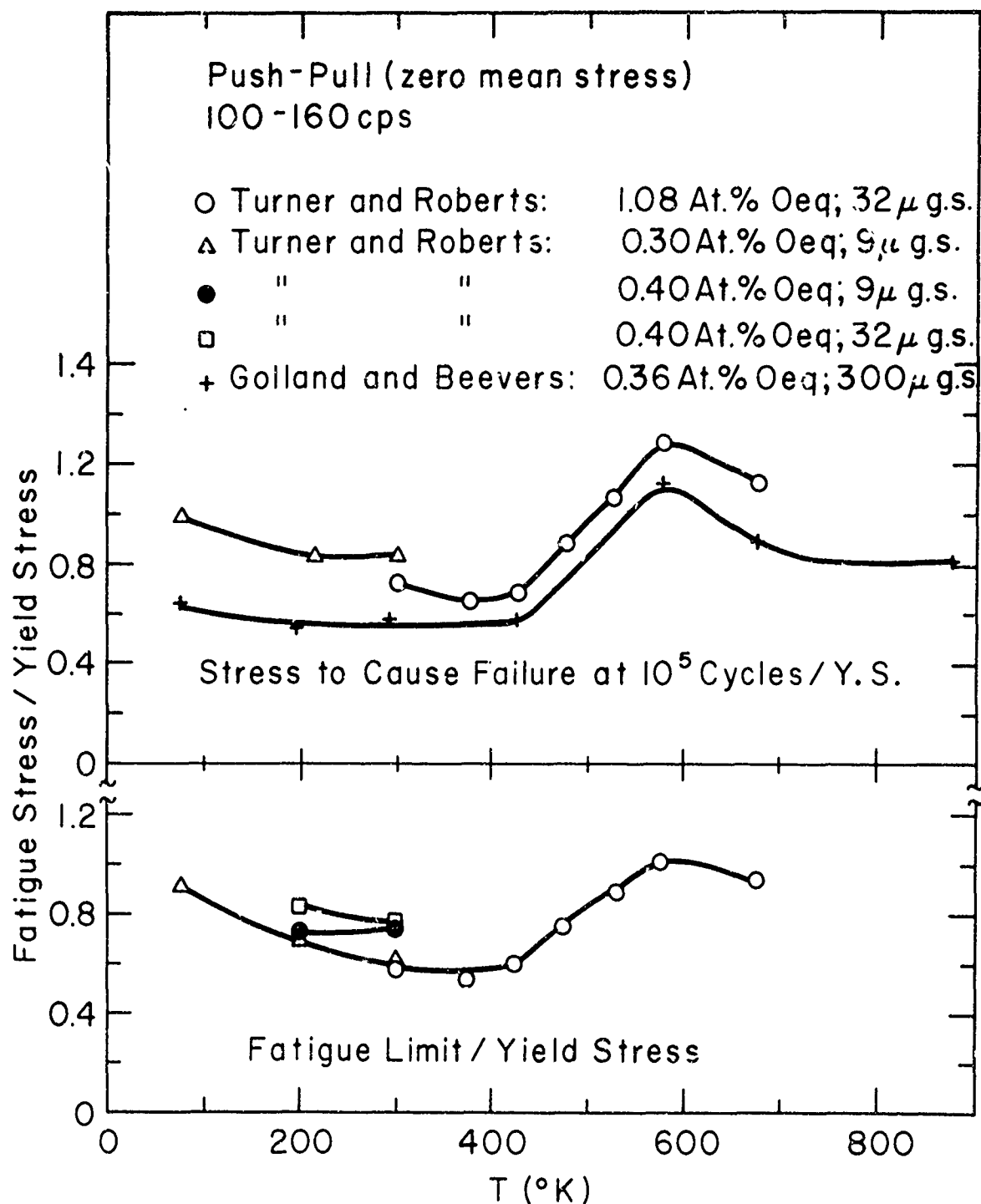


Fig. 23. Ratio of stress to cause failure at 10^5 cycles to the yield stress and ratio of the fatigue limit to the yield stress for unalloyed titanium as a function of temperature. Data from Refs. 99, 100 and 103.

References

1. Metals Handbook 8th Ed. Vol 1 (1961).
2. C. Kittell, Introduction to Solid State Physics, Wiley, N. Y. (1968).
3. E. W. Collings and J. C. Ho, The Science, Technology and Application of Titanium, Pergamon Press, N.Y. (1970) p. 331.
4. E. W. Collings, J. C. Ho and R. I. Jaffee, "Theory of Titanium Alloys for High Temperature Strength" Tech. Rept. AFML-TR-71-228 (Oct. 1971).
5. P. E. Armstrong and H. L. Brown, Trans. AIME 230 962 (1964).
6. E. S. Fisher and C. J. Reinken, Phys. Rev. 135 No. 2A, A482 (1964).
7. H. R. Ogden, D. J. Maykuth, W. L. Finlay and R. I. Jaffee, Trans AIME 197 267 (1953).
8. E. S. Fisher and D. Deven, The Science, Technology and Application of Titanium, Pergamon Press, N.Y. (1970) p. 373.
9. N. Hsu and H. Conrad, Scripta Met. 5 905 (1971).
10. M. Doner and H. Conrad, in preparation.
11. P. G. Partridge, Met. Reviews 118 169 (1968).
12. W. R. Tyson, The Science, Technology and Application of Titanium, Pergamon Press, N.Y. (1970) p. 479.
13. L. J. Teutonico, Ibid, p. 425.
14. A. D. McQuillan and M. K. McQuillan, Titanium, Academic Press, N. Y. (1956).
15. J. C. Williams and M. J. Blackburn, Phys. Stat. Sol. 25 K1 (1968).
16. T. R. Cass, The Science, Technology and Application of Titanium, Pergamon Press, N.Y. (1970) p. 459.
17. N. E. Paton and W. A. Backofen, Met. Trans. 1 2839 (1970).
18. C. S. Barrett and T. B. Massalski, Structure of Metals, 3rd Ed., McGraw Hill, N.Y. (1966).
19. N. E. Paton and J. C. Williams, 2nd Int. Conf. Strength of Metals and Alloys, Vol I. ASM (1970) p. 108.

20. J. F. Breedis and M. K. Koul, "Relationship of Structure to Strength in Titanium Alloys" Rept. AFML-TR-69-236 (June 1969).
21. H. S. Rosenbaum, Deformation Twinning, Gordon and Breach, N.Y. (1964) p. 43.
22. A. T. Churchman, Proc. Roy. Soc. A226 216 (1954).
23. H. Burrier, M. Amateau and E. Steigerwald, "The Relationship Between Plastic Deformation and Fracture in Alpha Titanium", Rept. AFML-TR-65-239 (July 1965).
24. E. Levine, Trans. AIME 236 1558 (1964).
25. C. Brehm and P. Lehr, Mein. Sci. Rev. Metallurg. 68 277 (1971).
26. T. Tanaka and H. Conrad, 2nd Int. Conf. Strength of Metals and Alloys, Vol I ASM (1970) p. 224.
27. T. Tanaka and H. Conrad, to be publ. Acta Met.
28. H. Conrad, Acta Met. 14 1631 (1966).
29. H. Conrad, AIME J. Met. 16 582 (1964).
30. T. Tanaka and H. Conrad, Acta Met. 19 1001 (1971).
31. S. Fujshiro and T. W. Edington, "Mechanical Twinning of Titanium Single Crystals", Tech. Rept. AFML-TR-70-176 (July 1970).
32. H. Conrad and H. Wiedersich, Acta Met. 8 128 (1960).
33. H. Conrad and I. Perlmutter, Conf. Int. Metallurgie Beryllium, Presses Univ. de France, Paris (1965) p. 319.
34. H. Conrad, G. London and V. Damiano, Anisotropy in Single Crystal Refractory Compounds, Plenum, N.Y. (1968) p. 153.
35. H. Conrad, High-Strength Materials, Wiley, N.Y. (1965) p. 436.
36. D. B. Snow and J. F. Breedis, 2nd Int. Conf. Strength of Metals and Alloys Vol II ASM (1970) p. 418.
37. K. Okazaki and H. Conrad, to be publ. Japan Inst. Met.
38. K. Okazaki and H. Conrad, submitted to Met. Trans.
39. H. W. Babel and S. F. Frederick, AIME Jour. Met. (Oct. 1968) p. 32.

40. C. Yin, M. Doner and H. Conrad, in preparation.
41. H. Hu and R. S. Cline, TMS-AIME 242 1013 (1968).
42. E. A. Calnan and C. J. B. Clews, Phil Mag. 41 1085 (1950);
ibid 42 616, 919 (1951); ibid 43 93 (1952).
43. D. N. Williams and D. S. Eppelsheimer, J. Inst. Met. 81 553
(1952-53).
44. R. Armstrong, I. Codd, R. Douthwaite and N. Petch, Phil.
Mag. 7 45 (1962).
45. G. Sachs, Zeit. d. ver. deut. Ing. 72 734 (1928).
46. K. Okazaki and H. Conrad, submitted to Acta Met.
47. S. N. Monteiro, A. T. Santhanam and R. E. Reed-Hill, The
Science, Technology and Application of Titanium, Pergamon,
N.Y. (1970) p. 503.
48. T. Tanaka and H. Conrad, in preparation.
49. A. M. Garde, A. T. Santhanam and R. E. Reed-Hill, Acta
Met. 20 215 (1972).
50. A. T. Santhanam and R. E. Reed-Hill, Met. Trans. 2 2619 (1971).
51. R. J. Wasilewski, Trans. ASM 56 221 (1963).
52. R. N. Orava, G. Stone, and H. Conrad, Trans ASM 59 171 (1966).
53. H. Conrad and R. Jones, The Science, Technology and Application
of Titanium, Pergamon, N.Y. (1970) p. 489.
54. H. Conrad, K. Okazaki, V. Gadgil, M. Jon, Electron Microscopy
and Strength of Materials, Univ. of Calif. Press, Berkeley (1972)
p. 438.
55. F. D. Rosi and F. C. Perkins, Trans ASM 45 972 (1953).
56. W. R. Kiessel and M. J. Sinott, Trans. AIME 197 331 (1953).
57. G. A. Sargent and H. Conrad, Scripta Met. 4 129 (1970).
58. R. Zeyfang and H. Conrad, Acta Met. 19 985 (1971).
59. K. Okazaki, T. Itoh and H. Conrad, in preparation.
60. B. deMeester, M. Doner and H. Conrad, in preparation.
61. S. F. Frederick and W. D. Nanna, "Kinetics of Cryogenic Plastic
Deformation of Ti-5Al-2.5Sn" Douglas Missiles and Space Systems
Div. DAC Rept. No. 59595 (Apr. 30, 1968).

62. R. L. Fleischer, *The Strengthening of Metals*, Reinhold Pub. Corp., N.Y. (1964) p. 93.
63. G. Sargent and H. Conrad, *Scripta Met.* 3 43 (1969).
64. R. Zeyfang, R. Martin and H. Conrad, *Met. Sci. Eng.* 8 134 (1971).
65. U. F. Kocks, *Canad. J. Phys.* 45 737 (1967).
66. J. Friedel, *Dislocations*, Addison-Wesley, Reading, Mass. (1965) p. 224.
67. J. Kratochvil and H. Conrad, *Scripta Met.* 4 815 (1970).
68. R. Jones and H. Conrad, *Trans. AIME* 245 779 (1969).
69. H. Conrad and K. Okazaki, *Scripta Met.* 4 111 (1970).
70. H. Conrad and K. Okazaki, *Scripta Met.* 4 259 (1970).
71. H. Conrad, *Mat. Sci. and Engr.* 6 265 (1970).
72. K. Okazaki and H. Conrad, to be published *Japan Inst. Met.*
73. H. Conrad, *Ultrafine Grain Size Metals*, Syracuse Univ. Press, Syracuse, N.Y. (1970) p. 213.
74. H. Wiedersich, *AIME J. Met.* 16 425 (1964).
75. H. Gegel, private communication.
76. R. Fowler and E. A. Guggenheim, *Statistical Thermodynamics*, Cambridge Univ. Press, London (1939).
77. O. Kubaschewski and H. A. Sloman, *The Physical Chemistry of Metallic Solid Solutions and Intermetallic Compounds*, 1 HMSO, London (1959) paper 3B.
78. E. N. Collings, H. L. Gegel and J. C. Ho, "Fundamental Design of Titanium Alloys", private communication.
79. Y. Lii, V. Ramachandran and R. E. Reed-Hill, *Met. Trans.* 1 447 (1970).
80. A. M. Garde and R. E. Reed-Hill, *Met. Trans.* 2 2885 (1971).
81. J. Weertman, *J. Appl. Phys.* 28 1185 (1957).
82. G. V. Kidson and R. Ross, *Radioisotopes in Scientific Research*, Pergamon, N.Y. (1958) p. 185.
83. C. Zener, *J. Appl. Phys.* 22 372 (1951).

84. H. J. Griest, A. M. Sabroff and P. D. Frost, Trans. ASM, 51 9351 (1959).
85. H. Bühler and H. W. Wagener, Bänder Bleche Rohre 6 677 (1965).
86. F. B. Cuff and N. J. Grant, Iron Age 170 134 (1952).
87. F. Garofalo, L. Zewell, A. S. Keh and S. Weissmann, Acta Met. 9 721 (1961).
88. A. D. Le Claire, Diffusion in BCC Metals, ASM (1965) p. 13.
89. M. F. Amateau, H. I. Burrier and L. J. Ebert, Trans. ASM 9 920 (1966).
90. H. I. Burrier, M. F. Amateau and E. A. Steigerwald, "The Relationship Between Plastic Deformation and Fracture in Alpha Titanium", Tech. Rept. AFML-TR-65-239 (July 1965).
91. R. L. Jones, F. W. Cooke, H. Conrad and B. R. Banerjee, "Investigations to Understand the Deformation and Strengthening Mechanisms of Solid Solution Phases of Titanium", Tech. Rept. AFML-TR-68-28 (Feb. 1968).
92. P. W. Bridgman, Trans. ASM 32 553 (1944).
93. L. Sama, O. J. Opinski and L. L. Seigle, "Tensile and Impact Properties of Commercial Titanium over the Temperature Range -196°C to 500°C, WADC Tech. Rept. 54-422 (Sept. 1954).
94. W. L. Finlay and J. A. Snyder, Trans. AIME 188 277 (1950).
95. R. I. Jaffee, H. R. Ogden and D. J. Maykuth, Trans. AIME 188 1261 (1950).
96. R. I. Jaffee and I. E. Campbell, Met. Progress 55 356 (1949).
97. R. L. Orr, O. D. Sherby and J. E. Dorn, Trans. ASM 45 113 (1954).
98. H. A. Lipsitt and D. Y. Wang, Trans. AIME 221 918 (1961).
99. N. G. Turner and W. T. Roberts, J. Less-Common Met. 16 37 (1968).
100. N. G. Turner and W. T. Roberts, Trans. AIME 242 1223 (1968).
101. J. Beevers and J. L. Robinson, J. Less-Common Met. 17 345 (1969).

102. D. I. Golland and C. J. Beevers, Met. Sci. Jnl. 5 174 (1971).
103. D. I. Golland and C. J. Beevers, J. Less-Common Met. 23 174 (1971).
104. S. L. Robinson, M. R. Warren and C. J. Beevers, J. Less-Common Metals, 19 73 (1969).
105. C. J. Beevers, The Science, Technology and Application of Titanium, Pergamon, N.Y. (1970) p. 535.
106. P. G. Partridge, Phil. Mag. 12 1043 (1965).
107. C. J. Beevers and M. D. Haliday, Met. Sci. Jnl. 3 74 (1969).

PUBLICATIONS

1. Scientific Journals

- * 1. R. L. Jones and H. Conrad, Acta Met. 15 649 (1967).
- * 2. R. L. Jones and H. Conrad, Scripta Met. 2 237 (1968).
- * 3. R. L. Jones and H. Conrad, TMS-AIME 245 779 (1969).
- 4. G. Sargent and H. Conrad, Scripta Met. 3 43 (1969).
- 5. G. Sargent, G. Jones and H. Conrad, Scripta Met. 3 481 (1969).
- 6. R. Tang, J. Kratochvil and H. Conrad, Scripta Met. 3 485 (1969).
- * 7. H. Conrad and R. Jones, The Science, Technology and Application of Titanium, Pergamon Press, N.Y. (1970) p. 489.
- 8. G. Sargent and H. Conrad, Scripta Met. 4 129 (1970).
- 9. J. Kratochvil and H. Conrad, Scripta Met. 4 815 (1970).
- 10. H. Conrad and K. Okazaki, Scripta Met. 4 259 (1970).
- 11. H. Conrad and K. Okazaki, Scripta Met. 4 111 (1970).
- 12. T. Tanaka and H. Conrad, 2nd Int. Conf. on Strength of Metals and Alloys, Vol. I, ASM (1970) p. 224.
- 13. H. Conrad, Mat. Sci. and Eng. 6 265 (1970).
- 14. J. Kratochvil and R. DeAngelis, J. Appl. Phys. 42 1091 (1971).
- 15. T. Tanaka and H. Conrad, Acta Met. 19 1001 (1971).
- 16. R. Zeyfang and H. Conrad, Acta Met. 19 985 (1971).
- 17. R. Zeyfang, R. Martin and H. Conrad, Mat. Sci. Eng. 8 134 (1971).
- 18. L. Rice, C. F. Hinesley and H. Conrad, Metallog. 4 257 (1971).

19. H. Conrad, K. Okazaki, V. Gadgil and M. Jon, Electron Microscopy and Structure of Materials, Univ. of Calif. Press, Berkeley (1972), p. 438.
20. K. Okazaki and H. Conrad, "Thermal and Athermal Components of the Flow Stress in Zone-Refined Titanium", to be published Trans. JIM, Japan.
21. K. Okazaki and H. Conrad, "Grain Size Distribution in Recrystallized Alpha-Titanium", to be publ. Trans. JIM, Japan.
22. K. Okazaki, M. Momachi and H. Conrad, "Grain Growth Kinetics in Ti-N Alloys", to be publ. 2nd Int. Conf. on Titanium, Cambridge, Massachusetts, May 2-5, 1972.
23. K. Okazaki, M. Momachi and H. Conrad, "Thermally Activated Deformation on Ti-N Alloys", *ibid.*
24. H. Conrad, M. Doner and B. deMeester, "Plastic Flow and Fracture of Titanium", *ibid.*
25. K. Okazaki and H. Conrad, "Recrystallization and Grain Growth in Alpha Titanium: I Characterization of the Structure", submitted to Met. Trans.

* Work performed under Air Force Contract AF33(615)-3864.

2. Theses

1. Pasupathy Ganesan, "Grain Growth in Ti-4 Wt. % Al and Ti-26 Wt. % Mo Alloys", M. S. Thesis, University of Kentucky (1970).
2. Min Chung Jon, "Effect of Grain Size on the Dislocation Density of High Purity Titanium Deformed at Different Temperatures", M. S. Thesis, University of Kentucky (1971).
3. Vishwas Vinayak Gadgil, "Effect of Grain Size on the Dislocation Density of Titanium (0.2 At. % O_{eq}) Deformed 78°K to 500°K", M. S. Thesis, University of Kentucky (1971).